Mauet Medical

Mechanical Heart Valve Design

Final Report

Team members

Theresa-Lynne Danielle Filio (0703256)

Taimoor Khan (0707108)

Peter Morreale (0729149)

Vasudha Kalia (0740392)

Faculty Advisor- Dr. John Runciman, Ph.D, P.Eng

Course Coordinator- Dr. Richard Zytner, Ph.D, P.Eng

School Of Engineering

University of Guelph

Executive Summary

The human heart is one of the most complex mechanisms in the body. It plays a very crucial role in the uni-directional flow of blood. It is very important for the human body that the heart continues to pump blood sufficiently. The heart has four valves that regulate the transportation of blood. A defect in these valves can result in serious conditions such as stenosis of the valvular opening, prolapse or regurgitation of blood forcing the heart to work harder to pump blood [1]. Each year over 250,000 individuals undergo heart valve replacement surgery due to heart valve disease [2]. The continuous ongoing research has provided several advancements in heart valve replacement over the past few decades. Artificial heart valves are usually categorized into two categories, tissue and mechanical. This project involves the design, modeling, and experimentation of a mechanical heart valve model that serves as a successful alternative to an existing heart valve design by improving upon their associated problems or risks such as turbulence and its impact against other anatomical structures of the heart. The chosen design was a tri-leaflet valve that was designed and 3-D modeled on SolidWorks. It was then analyzed using Computational Fluid Dynamics (CFD) and Finite Element Analysis (FEA) by creating 2-D cross sections. These analyses showed that the flow across the valve and its ability to withstand pressures were comparable to other studies. The model was then 3-D printed in ABS plastic and tested on the ex vivo horse heart and lung simulator. The simulator tested pressure difference, flow behaviour and turbulence. It was found that the valve was able to withstand pressures that were close to physiological pressures. The valve was then redesigned and 3-D printed into medical grade stainless steel 316L. When designing the valve the design was put within the structural housing and the amount of small structures were limited. Some constraints for this project include durability for long term implementation, making sure the seal of the valves remains completely shut, and minimizing turbulence and backflow.

Deliverables of the 3-D printed models in ABS plastic and a tri-leaflet model printed in medical grade stainless steel 316L will be submitted with this final report by December 1st 2014.

Table of Contents

Table of Figures

Table of Tables

1.0 Introduction to Design

1.1 Problem Statement

The human heart works on a very complex mechanism where the valves play a crucial role in the one directional flow of the blood. The human heart consists of four chambers, between which the valves regulate the transportation of blood. A defect in a valve can result from various conditions such as stenosis of the valvular opening, prolapse or regurgitation of blood within the chambers forcing the heart muscles to work harder to pump blood throughout the body and maintain a normal blood pressure [1]. Many symptoms associated with valve defects include angina, palpitations, shortness of breath and swelling. This can in turn lead to heart failure and eventual death. According to a study at the University of California, San Francisco, there are 250,000 people coping with different kinds of valvular diseases and the only treatments available are medications to reduce the rate of degradation of the valve or surgical repair and replacement of the valve. In several cases, valve replacement becomes a necessity to prevent the heart failure [2]. The purpose of this project is to design a mechanical heart valve to serve as a replacement to a natural human heart valve and restore the correct functioning of said valve.

The scope of this project was to design, model, and experimentally test a mechanical heart valve model that serves as a successful alternative to existing heart valve designs by improving upon their associated problems or risks. A functional prototype will be printed from medical grade stainless steel 316L as a final deliverable upon project completion. This project will also open up development opportunities for future University of Guelph engineering students.

The amount of people with heart valve defects or degradation has increased the incidents of surgical replacements, which highlights the need for successful artificial valves [2]. There are 5 types of artificial valves available: caged ball valve, non-tilting valve, tilting valve, bileaflet valve, and polymeric valve. *Table 8* effectively summarizes the advantages and disadvantages of the types of mechanical valves available in the market. The criteria and constraints stated in this document have been chosen to include the advantages of these designs along with an attempt to eliminate disadvantages of current heart valves.

1.2 Objectives

The main goal of the report was to design and model two different prototypes in SolidWorks and eventually choose the most suitable design through several analysis techniques including: computational fluid dynamics (CFD), finite element analysis (FEA) and sensitivity tests. An experimental simulation was also carried out on the designs in a heart and lung simulator. These experimental prototypes were composed of 3D printed ABS plastic and the final prototype was printed in medical grade stainless steel 316L.

2.0 Background to Problem

2.1 Cardiovascular Anatomy Background

2.1.1 Cardiovascular System and the Heart

The main purpose of the cardiovascular system is transporting blood throughout the body [3]. Blood is composed of erythrocyte, leukocyte and thrombocyte cells that carry nutrients, oxygen, waste products, and carbon dioxide which are needed by or disposed from cells in the body [4]. Blood is pumped through two different subsystems of the cardiovascular system, the pulmonary and systemic systems, by the heart [3], [5].

The heart has four chambers that operate together as a double pump [3]. As seen in *Figure 1* each side of the heart is composed of an atrium and ventricle that pumps blood to its designated location. The human heart also contains four valves that prevent backflow through the organ [3]. They consist of the tricuspid valve, the mitral valve, the pulmonic valve and the aortic valve [6]. These valves will be discussed in further detail in *Section 2.1.2 Valve Anatomy*.

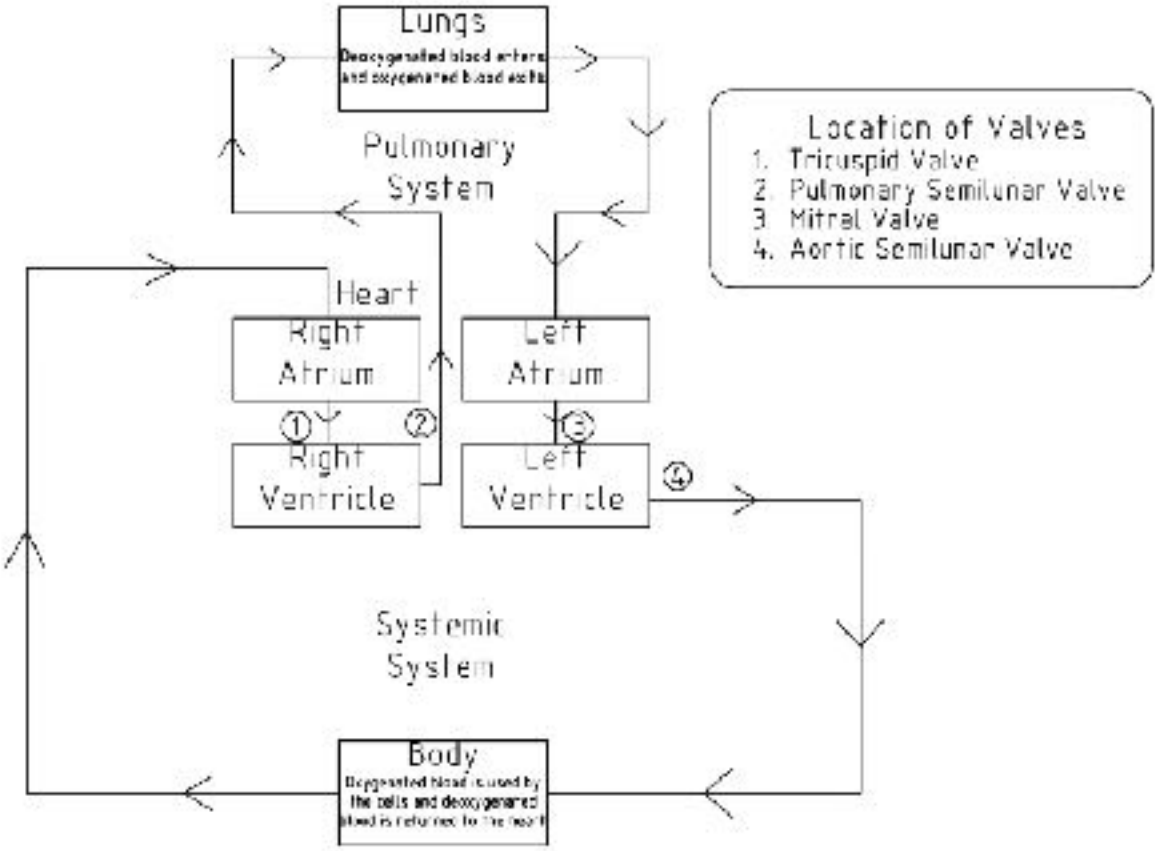

FIGURE 1: SCHEMATIC OF CARDIOVASCULAR SYSTEM

Deoxygenated blood from the body enters the right side of the heart through the vena cavae [3], [5]. It then passes through the right side of the heart where it is pumped towards the lungs through the pulmonary arteries [3], [5]. The lungs exchange carbon dioxide in the blood with oxygen and return the now oxygenated blood to the left side of the heart through the pulmonary veins [3], [5]. The blood then flows through the left side of the heart where it is pumped into the rest of the body through the aorta [3], [5].

2.1.2 Valve Anatomy

As mentioned *in Section 2.1.1 Cardiovascular System and the Heart*, a human heart contains four heart valves: the tricuspid, mitral, pulmonic and aortic valves [6]. The purpose of these valves is to control the flow of blood through the heart chambers ensuring unidirectional flow [3]. When one or more the heart's valves do not function properly, it may lead to severe

complications and even death, which will be further discussed in *Section 2.1.3 Valve Deformations and Diseases*.

The valves of the heart can be divided into two categories: atrioventricular and semilunar valves [3], [6]. The atrioventricular valves control the flow between the atria and the ventricle and consist of the tricuspid and mitral valves [3], [6]. The tricuspid valve is located on the right side of the heart while the mitral valve is located on the left side [3], [6]. These valves operate with the help of the chordae tendineae and the papillary muscles in the ventricle [7]. The chordae tendineae are attached on one end to the leaflets of the atrioventricular valve and to the papillary muscles on the other end [7]. The papillary muscles, which are attached to the ventricle wall, contract during ventricular contraction to ensure the leaflets remain closed [7]. The semilunar valves control the flow between the ventricle and the artery exiting the heart and consist of the pulmonic and aortic valves [3], [6]. The pulmonic valve is located between the right ventricle and the pulmonary artery while the aortic valve is between the left ventricle and the aorta [3], [6].

The tricuspid, pulmonic and aortic valves all consist of three leaflets while the mitral valve only has two [3]. The average dimensions of a healthy, adult human heart are summarized in *Table 1* below.

TABLE 1: AVERAGE DIMENSIONS OF HUMAN HEART VALVES

Characteristic	Tricuspid	Mitral	Aortic	Pulmonic
Circumference (cm)	11.63	9.79	7.28	7.63
Area (cm^2)	7.76	10.56	4.56	4.71
Diameter (cm)	3.11	3.64	2.32	2.43

*Dimensions were obtained from the experiments conducted by Westaby et *al.* [8].

The operation of these valves are dependent on the changes in pressure across the atrium and ventricle [9]. Within the duration of one heartbeat, the heart goes through two phases: systole and diastole [3]. When in systole, the ventricle contract, causing the ventricle's pressure to increase [3], [9]. When the ventricle's pressure is greater than the atria, pulmonary artery and

aorta, the atrioventricular valves (tricuspid and mitral valves) close while the semilunar valves (pulmonic and aortic valves) open pumping blood out of the heart [3], [9]. When in diastole, the ventricles relax reducing the pressure in the ventricles [3], [9]. When the ventricle's pressure is lower than the atria, pulmonary artery and aorta, the atrioventricular valves open while the semilunar valves close allowing the heart to refill with blood [3], [9]. At the end of the diastolic phase, the atria contract to empty its blood into the ventricle before the cardiac cycle repeats itself [3]. The pressures in the atria, ventricles, pulmonary artery and aorta during systole and diastole can be found in *Table 2* below.

TABLE 2: AVERAGE PRESSURES OF HEART COMPONENTS DURING SYSTOLE AND DIASTOLE

	Systole	Diastole
Position of Atrioventricular Valves	close	open
Position of Semilunar Valves	open	close
Pressure of Right Ventricle (mm Hg)	25	5
Pressure of Left Ventricle (mm Hg)	120	10
Pressure of Right Atrium (mm Hg)	5	5
Pressure of Left Atrium (mm Hg)	10	10
Pressure of Pulmonary Artery (mm Hg)	25	10
Pressure of Aorta (mm Hg)	120	70

*Average pressure values were obtained from reference [10].

The cardiac cycle of an adult repeats itself approximately 75 times per minute [3]. Thus the heart valve must not only be able to withstand the pressure drops of the heart but also cyclic fatigue. The general composition of heart valves are 43-60 wt% of collagen, 10-13 wt% elastin and 20 wt% glycosaminglycans [11]. A study by *Barber et al.*, (2001) conducted tensile strength testing on healthy and diseased human mitral valves and found that the average mechanical characteristics of a the healthy valves include a percent elongation of 17.3%, a stiffness of 6.1 kPa and a tensile strength of 801 Pa [12].

2.1.3 Valve Deformations and Diseases

As seen in *Section 2.1.2 Valve Anatomy*, heart valves play a vital role in the proper functioning of the heart, however, deformations or diseases can occur that decrease the ability of the valve to function properly. Failure of the heart valve, also known as valvular heart disease, can lead to either valvular stenosis or valvular regurgitation [13]. Valvular stenosis is defined as the narrowing of the heart valve and the heart must work harder to counter the decrease in blood flow [13]. Valvular regurgitation occurs when the leaflets are unable to close, increasing the risk of blood backflow [13].

Mitral Valvular Diseases

The main mitral valvular diseases are mitral regurgitation mitral stenosis and mitral valve prolapse [14]. Mitral valve prolapse can be caused genetically (ie. an individual may have the chromosomal traits for Marfan syndrome whose effects can cause mitral valve prolapse) and severe cases typically lead to mitral regurgitation [14]. Mitral regurgitation is more prevalent in males while occurrence of mitral stenosis is typically seen in females [14], [15].

The main cause of mitral stenosis is rheumatic fever which is prevalent in children aged five to fourteen [14], [16]. After the fever affects the valve (effects summarized in *Table 3*), the state of the valve worsens over a span of years (typically between 40 and 50 years) [14], [16]. Approximately 40% of individuals who become ill with rheumatic fever develop both regurgitation and stenosis in the mitral valve [14]. Medications are available to decrease the severity of the disease and prolong the need for surgery [14].

TABLE 3: SUMMARY OF VALVULAR DISEASES IN THE MITRAL VALVE

	Mitral Regurgitation	Mitral Stenosis	Mitral Valve Prolapse
Causes	- prolapse - rheumatic fever -annular calcification -ischemic heart disease	- rheumatic fever	- Marfan syndrome -Ehlers-Danlos syndrome -hyperthyroidism
Effects to Heart Structures	- deformation of the chordae tendineae - abnormal function of the papillary muscles - decrease in ventricle radius	- thickening of leaflets - decrease in valve diameter - merging of leaflets -calcification of leaflets -deformation of the chordae tendineae	- in young females, the leaflets become thinner -in elderly males (aged >50), the leaflets become thicker - in both cases the leaflets weaken or become flail - elongation or deformation of the chordae tendineae -friction lesions in the ventricle
Effects to Cardiovascular System	- decrease in end systolic ventricular pressure - increase in end diastolic volume of left ventricle -decrease in cardiac output	- if cardiac output is normal, the pressure drop between left atrium and ventricle increases - if cardiac output decreases, the pressure drop between the left atrium and ventricle decreases	- decrease in overall blood pressure

Physical Symptoms	- chronic weakness - fatigue	- dyspnea -chest pain -irregular heart beat	- typically asymptomatic -systolic click - dyspnea -fatigue - chest pains
Treatment Options	- medications such as beta-blocking drugs or ACE inhibitors - valve repair -valve replacement	- mitral valvotomy - valve replacement	- similar to treatment for mitral regurgitation - valve replacement

*The characteristics of mitral valvular disease were obtained from [14] - [16].

Tricuspid Valvular Disease

The main tricuspid valvular diseases are tricuspid regurgitation and tricuspid stenosis [14]. Typically when a person has a tricuspid valvular disease, a mitral valvular disease is also present [14]. A summary of the characteristics of tricuspid valvular diseases can be found in *Table 4* below.

TABLE 4: SUMMARY OF VALVULAR DISEASES IN THE TRICUSPID VALVE

	Tricuspid Regurgitation	Tricuspid Stenosis
Causes	- rheumatic fever - carcinoid syndrome -Ebstein anomaly - right ventricle failure - primary pulmonary hypertension - papillary muscle dysfunction - tricuspid valve prolapsed	- rheumatic fever - right atrial tumors - congenital tricuspid atresia
Effects to Heart Structures	- dilation of the right side of the heart including tricuspid valve	- thickening of leaflets - decrease in valve diameter
Effects to Cardiovascular System	- increase in diastolic volume in right ventricle	- low cardiac output - increase in systemic venous pressure
Physical Symptoms	- weight loss -cachexia - jaundice - cyanosis - discomfort in neck	- fatigue -anorexia -edema -discomfort in neck
Treatment Options	- valve replacement	- decrease in sodium intake -open valvotomy - valve replacement

* The characteristics of tricuspid valvular disease were obtained from [14].

Aortic Valvular Diseases

The main aortic valvular diseases are aortic regurgitation and aortic stenosis [14]. Aortic stenosis can occur in one or more of the aortic valves three leaflets [14]. Aortic valvular diseases are more prevalent in men [14]. These diseases can cause endocarditis which are responsible for

approximately 1200 deaths per year in the United States [14]. The characteristics of aortic valvular diseases are summarized in *Table 5* below.

TABLE 5: SUMMARY OF VALVULAR DISEASES IN THE AORTIC VALVE

	Aortic Regurgitation	Aortic Stenosis
Causes	- rheumatic fever - aortic root disease - infective endocartitis - calcific aortic stenosis	- rheumatic fever - calcification of the mitral valve - calcification of the tricuspid valve
Effects to Heart Structures	- thickening of the left ventricle	-increase in muscle mass and stiffness of the left ventricle
Effects to Cardiovascular System	- increase in blood volume and blood pressure in the left ventricle	- increase in diastolic pressure in the left ventricle - increase in systolic pressure - increase in oxygen demand for the left side of the heart
Physical Symptoms	- angina pectoris - myocardial ischemia	- dyspnea - angina pectoris - heart failure
Treatment Options	- vasodilator therapy - valve replacement	- balloon aortic valvotomy for infants - valve replacement for adults

* The characteristics of aortic valvular disease were obtained from [14].

Pulmonic Valvular Diseases

The main pulmonic valvular disease is pulmonic regurgitation although stenosis to the pulmonic valve can also occur [14]. Most often pulmonic valve diseases are not severe enough to cause significant problems making pulmonic valve replacements a rare occurrence [14].

TABLE 6: SUMMARY OF VALVULAR DISEASES IN THE PULMONIC VALVE

	Pulmonic Regurgitation
Causes	- dilation of the pulmonic valve - dilation of the pulmonary artery - infective endocarditis
Effects to Heart Structures	- enlarged pulmonary artery
Effects to Cardiovascular System	- increase in blood volume in the right ventricle
Physical Symptoms	- Graham Steell murmur
Treatment Options	- valve repair - valve replacement

* The characteristics of pulmonic valvular disease were obtained from [14].

2.2 Previous Designs and Analyses

2.2.1 Previous Designs

Section 2.1.3 Valve Deformations and Diseases outlined the severity of decreased heart valve functionality, highlighting the importance of development of methods of treatment. Primary methods of treatment include medications but if it can no longer manage the disease, the valve would need to be surgically repaired or replaced [17]. Heart valve surgeries have been conducted since the early 1900s with the first heart valve repair performed in 1923 by Dr. Elliot Cutler in Boston [18]. Over the years, the practice has developed and valves can also be replaced if they are beyond surgical repair. The first heart valve replacement procedure was conducted by Dr. Charles Hufnagel in 1952 using a caged ball valve design [19]. Heart valve replacements can be divided into two categories: tissue (biological) valves and mechanical valves [20]. *Table 7* below compares the advantages and disadvantages of tissue valves and mechanical valves.

TABLE 7: COMPARISON OF MECHANICAL AND BIOLOGICAL HEART VALVES

	Mechanical Heart Valves	Biological Heart Valves
Advantages	- greater durability	- lower risk of thromboembolism
Disadvantages	- greater risk of thromboembolism	- greater risk of structural deterioration

* Advantages and disadvantages obtained from [14].

Due to the scope of the project, the history of mechanical heart valves will be focused on in greater detail. Currently mechanical heart valve designs can be characterized as caged ball valves, non-tilting disc valves, tilting disc valves, bi-leaflet valves, and polymeric valves [19], [21]. *Figure 2* depicts a timeline for the creation of past mechanical heart valve designs and *Table 8* summarizes the main characteristics including the advantages and disadvantages of each type of valve.

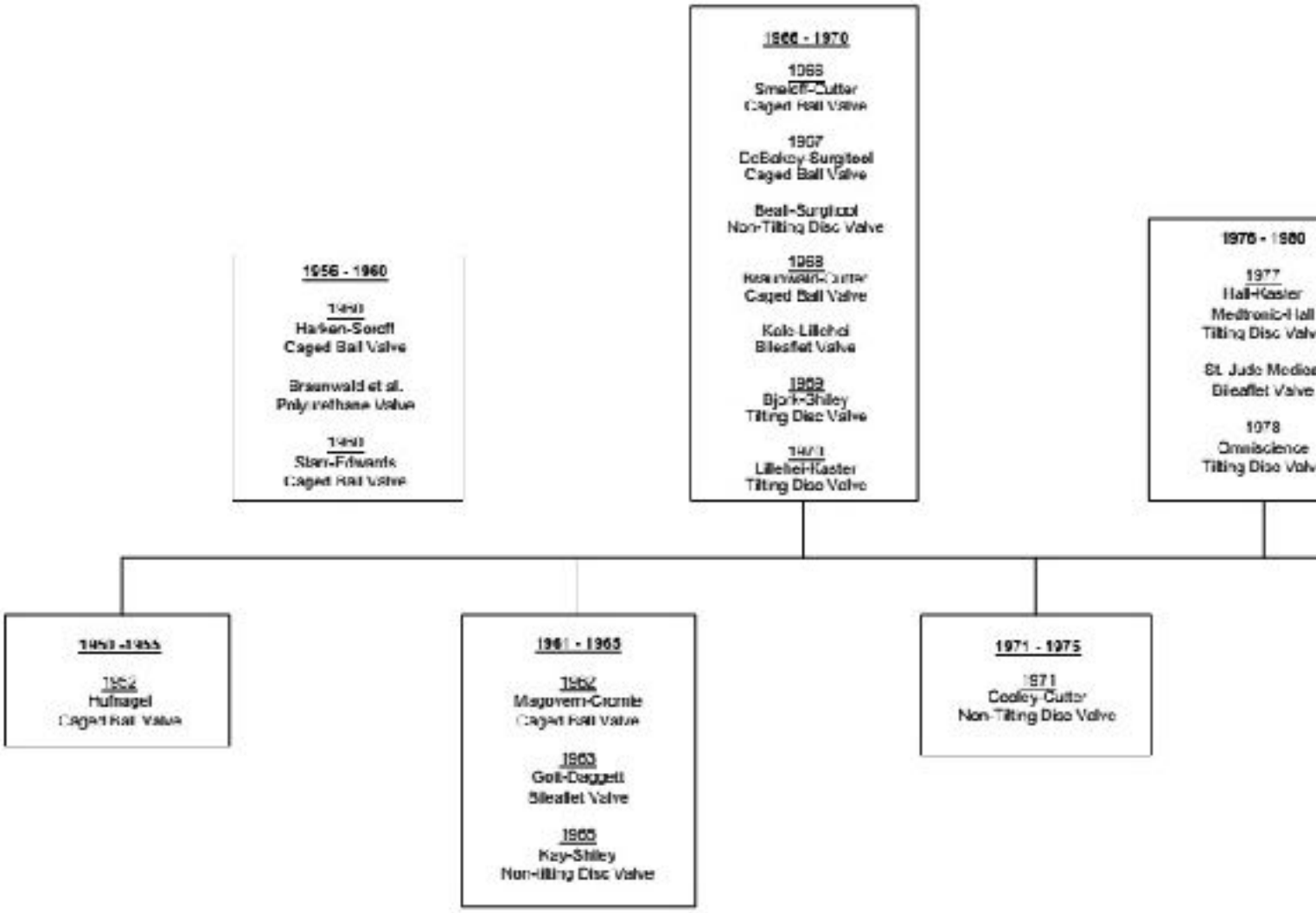

*Information for this timeline was obtained from [19], [25].

FIGURE 2: TIMELINE OF PREVIOUS MECHANICAL HEART VALVES

TABLE 8: SUMMARY OF PREVIOUS MECHANICAL HEART VALVE DESIGNS

	Caged-Ball Valves	Non-Tilting Valves	Tilting Valves	Bileaflet Valves	Polymeric Valves
Previous Designs	- Hufnagel Ball Valve *obsolete - Starr-Edwards Ball Valve	-Kay-Shiley Disc Valve	- Omniscience Tilting Disc Valve - Omnicarbon Tilting-Disc Valve - Hall-Kaster and Medtronic-Hall Tilting Disc Valve	- St. Jude Medical Bi-Leaflet Valve - Carbomedics Bi-Leaflet Valve	- Polyethylene terephthalate Valves -Polyeurethane Valves
Components	- Ball - Cylindrical cage	- Disc - Cage	- Disc - Struts	- Leaflets - Hinges	- Biosynthetic Materials
Advantages	- Durability	- Less bulky than caged-ball	- Less coagulation than caged-ball and non-tilting	- Less coagulation	- Least likely to coagulate due to hydophobicity and neutral charge
Disadvantages	- Bulky - Noisy - High coagulation occurrence	- Less durable than caged-ball	- Coagulation along struts	- Hinge failure - Cavitation	- Calcification

*Data in this table was compiled using information from references [19]-[24].

2.2.2 Previous Materials and Analyses

Only a select number of materials are suitable for heart valve design as they would need to be durable and biocompatible for the human body. Three materials have been selected as

viable options for the design of this heart valve; pyrolytic carbon, a titanium-nickel alloy (Ti6Al4V) and stainless steel 316L. The physical and mechanical characteristics of these materials are summarized in *Table 9* below.

TABLE 9: COMPARISON OF MATERIALS SUITABLE FOR HEART VALVE DESIGN

Property	Stainless Steel 316L	Ti6A4V	Pure Pyrolytic Carbon
Composition (wt%)	Iron: 68.18 Chromium: 17.2 Nickel: 10.9 Molybdenum: 2.1 Manganese: 1.6 Carbon: 0.02	Titanium: 87.7 Aluminum: 6.0 Vanadium: 4.0	Carbon Hydrogen Note: Hydrocarbon undergoes pyrolysis (thermal decomposition) in anaerobic conditions
Density (g/cm^3)	8	4.43	1.85-2.10
Poisson's Ratio	0.25	0.342	0.3
Modulus of Elasticity (GPa)	193	113.8	23-29
Yield Strength with a 0.2% offset (MPa)	Hot finished and annealed: 170 Cold finished and annealed: 310	Annealed:830 Heat-treated and aged: 1103	
Tensile Strength(MPa)	Hot finished and annealed: 480 Cold finished and annealed: 620	Annealed: 900 Heat-treated and aged: 1172	100-120
Flexural Strength (MPa)			493.7
Percent Elongation (%)	50	Annealed: 14 Heat-treated and aged: 10	1.58
Fracture Toughness (MPa√m)	2.5	44-66	1.68
Thermal Conductivity (W/m*K)	At 100°C: 16.3	At 25°C: 6.7	3.4-13.5
Specific Heat (J/kg*K)	From 0-100°C: 500	At 25°C: 610	712
Electrical Resistivity (Ω*m)	$7.4x10^{-7}$	$17.1x10^{-7}$	$14.0x10^{-6}$

*Data from this table was taken from information from references [26]-[34].

Pyrolytic Carbon

Pyrolytic carbon has been used as material for mechanical heart valve production since 1968 and is still widely used to date [26]. It is a ceramic material that is made through the use of a fluidized-bed reactor that simulates anaerobic conditions [26], [27]. Hydrocarbons undergo the process of pyrolysis, which is defined as thermal decomposition [26]. Pyrolytic carbon can be mixed with other elements during this process to decrease variability, however pure pyrolytic carbon is the most desirable result due to better mechanical properties [26].

The reasons why pyrolytic carbon remains a popular choice as a mechanical heart valve material include its biocompatibility with blood and the human system, its thromboresistivity and its durability [26], [27]. As seen in *Table 9* the density of pyrolytic carbon is the lowest which is desirable because it allows for better flexibility of movement under the pressure gradient but its low percent elongation indicates that it does not deform and fracture easily [26]. Even though it is more biocompatible than other metals or ceramics, it still causes some coagulation to occur causing patients to require some degree of anticoagulation therapy [26].

Titanium-Nickel Alloy (Ti6Al4V)

Titanium metals have also been used in the fabrication of mechanical heart valves. The titanium-nickel alloy being considered is Ti6Al4V. This alloy has typically been used for the housing due to its high strength [28]. Its other advantages are its low density and its high corrosion resistance [28]. One of the main disadvantages of this alloy is that some patients are allergic to titanium metals [28]. Studies have been conducted to minimize this risk by applying a coating on top of the titanium-nickel layer [28]. For example a study by *Jozwik and Karczemska*, (2007) conducted tests on a heart valve made from Ti6Al4V but with a nanocrystalline diamond coating [28]. They found that this material was able to withstand long-term fatigue testing [28].

Medical Grade Stainless Steel 316L

The final material that was considered for mechanical heart valve production is medical grade stainless steel 316L. Currently this material has been widely used for joint replacements

due to its high strength but is now being considered as a viable option for mechanical heart valves [29]. Stainless steel 316L has a lower carbon content than stainless steel 316 which increases its resistance to corrosion making it more favourable for implanted devices [29]. Due to the availability of materials for this project, the final design will be 3-D printed in stainless steel 316L.

2.2.3 Previous Modelling Methods

A computational fluid dynamics analysis or CFD is a simulation that simulates liquid or gas passing through or around an object [35]. The analysis can be very complex, for instance, it can be used to measure unsteady and compressible flow, and heat transfer [35]. In the past CFD has been used to analyze the flow of blood through valves during leaflet movement [36]. A study by *Kelly,* (2002) used CFD to analyze their modifications on the housing of a bileaflet valve [36]. He looked at the moment of the leaflet under specific pressures and blood flow [36].

Finite element analysis or FEA is a SolidWorks simulation method that calculates displacements, strains and stresses under internal and external loading conditions [37]. In the past FEA has been used to analyze the stress applied to valve leaflets and to determine the possible locations for failure [38]. A study by *Smuts et al.,* 2010 used FEA to analyze the stresses on their aortic heart valve by simulating specific loads [38].

2.2.4 Previous Testing Methods

An important factor to analyze when physically testing a heart valve model is its durability. It is not only required to withstand physiological pressures but must be able to withstand cyclic loading for a long duration of time. A small angle light scattering device (SALS) can be used to test biological valves which was done in a study by *Wells, Sellaro, and* Sacks, (2005) [39]. This system uses light to determine the change in length of collagen fibres when exposed to various pressures [39]. For mechanical heart valves, its fatigue and durability can be assessed using a Rockwell Hardness test that will measure the permanent deformation of the valve under various pressures [40]. When testing a physical model of a heart valve, another important factor to assess its biocompatibility. A study by *Glasmacher, Nellen, Reul & Rau*,

(1999) used a Thrombolytic Assessment System and a Partial Thromboplastin Time measurement system to determine when coagulation occurs when interacted with the valve [41].

2.3 Standards and Protocols

2.3.1 Medical Devices Regulations

All medical devices are classified into one of Class I to IV by means of classification rules set out in the Medical Devices Regulation Act SOR/98-282. All medical devices shall not adversely affect the health and safety of the patient or user, except when those risks constitute acceptable risks when weighed against the benefits that the device brings [42]. All materials used in the manufacture of the medical device must be compatible with the other materials present and shall not pose any undue risk to the patient or user [42].

According the rule 1 of Medical Devices Regulations (SOR/98-282) any type of surgically invasive device is considered to be a class II device, if that device is intended to be absorbed by the body or that is normally intended to remain in the body for at least 30 days then it is classified as Class III, lastly if that device is intended to diagnose, monitor, control or correct a defect of the central cardiovascular system or the central nervous system or of a fetus in uterus it is then classified as class IV [42].

Any type of artificial heart valve is considered to be an implant and a Class IV medical device because of its invasive nature, it remains in the body for at least 30 days, and its intent to control or correct a defect in the cardiovascular system respectively [42].

This design will be Class IV medical device. It will be a surgically invasive device that will be used to correct a defect in the cardiovascular system, and will be intended to remain in the patient's body throughout the remainder of their life.

2.4 Constraints and Criteria

Taking into consideration the scope of the design, the constraints and criteria have been laid out so that they can be evaluated and applied to the developing models. For example the design must be able to withstand backflow pressures so systolic and diastolic pressures will be simulated against the design in the heart and lung simulator (described further in *Section 3.4.3*

Experimental Testing). Some of the constraints and criteria will be met through research, such as the device meeting medical regulations laid out by the Government of Canada or documented back flow pressures from journal articles. A discussion of how the chosen design meets the constraints and criteria listed below can be found in *Section 4.2 Constraints,* and *Section 4.3 Criteria.*

2.3.1 Constraints

- The design must follow all medical regulations of a Class IV medical device.
- The design must be durable for long term implementation.
- When closed, it must form a complete seal.
- It must withstand backflow pressure.
- Minimize turbulence in order to prevent damage to blood cells.
- Materials must be biocompatible.
- Must match or exceed functionality of existing designs.

2.3.2 Criteria

- Contain the design within the structural housing.
- Reduce cavitation on surfaces by limiting turbulence over surfaces.
- Minimize pressure drops across valve.
- Choose materials to eliminate absorption of proteins or other blood components.
- Limit small structural moving components in design.

2.5 Considerations

When designing a mechanical heart valve considerations in patient health and safety, materials, cost and time should be taken into account. A heart valve that is ready for implantation should meet the criteria of a class IV medical device (discussed in further detail in *Section 2.3.1 Medical Devices Regulations*). The Ministry of Health Canada also recognizes the standards for cardiovascular implants including cardiac valve prostheses from the International Standardization Organization (ref standards website). The valve should be designed to increase the longevity of the patient and should not cause harm after implantation. The material used for

the valve should also be taken into consideration to ensure that it is biocompatible with the body and can withstand physiological conditions. Methods to increase the biocompatibility of the valve can be found in *Section 4.5 Manufacturing*. While the cost of material is an important consideration for the design, it is important to ensure that this does not impede the health and comfort of the patient. The final consideration is time. This project was completed within the span of 12 weeks. Further research and testing must be done before the valve can be ready for implantation in human patients. Recommendations on how to take this project further can be found in *Section 6.0 Recommendations*.

3.0 Design Methodology

3.1 Stages of Design

In order to design a functional prototype a number of sketches and models were created in order to refine the design by making modifications based on results and client feedback. The tri-leaflet design underwent two sketching changes, a SolidWorks model review, a redesign based on the experimental apparatus, and finally a scale model was designed and prototyped based on the analysis results. A flow diagram of these models can be seen in the following figure.

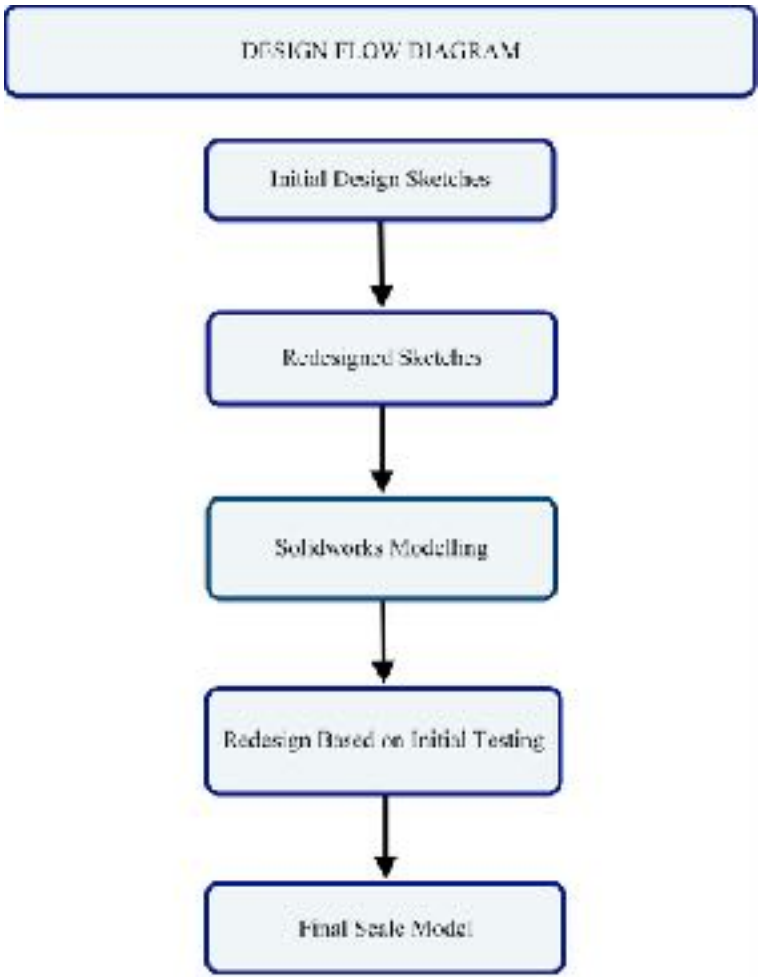

FIGURE 3: FLOW DIAGRAM OF DESIGN PROCESS

Top View	Orthonormal View

3.1.1 Initial Design Sketch

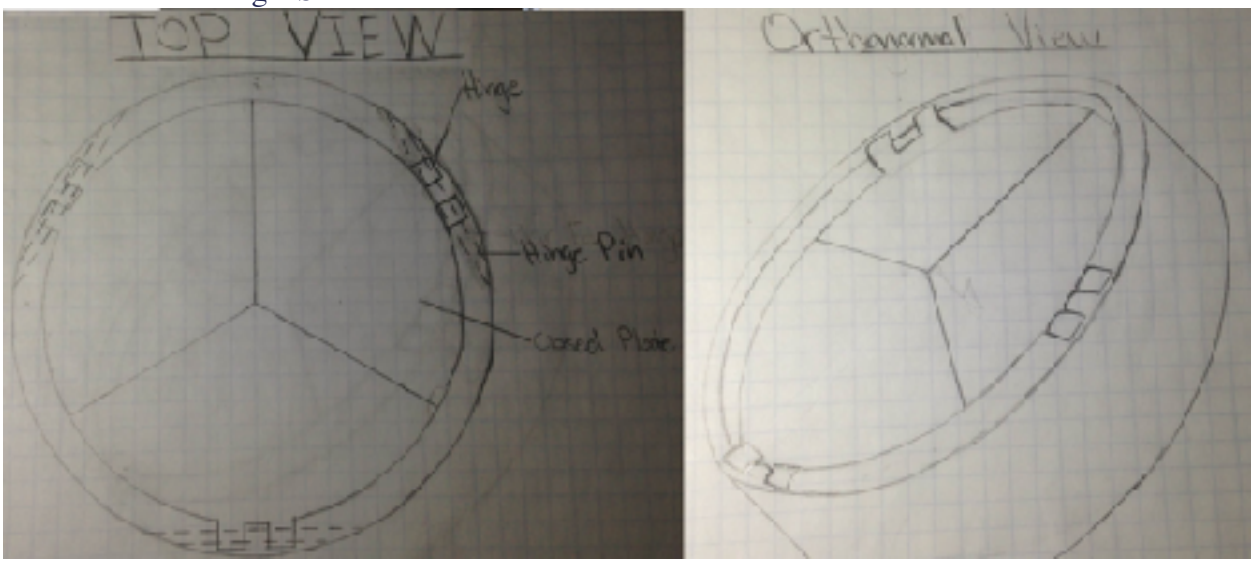

FIGURE 4: SKETCHES OF INITIAL TRI-LEAFLET DESIGN

The original design consisted of a cylindrical housing and three leaflets. The leaflets or plates consisted of a flat top and bottom surface with hinge connectors on the edge of the housing. The leaflets were held in place by a pin which would be inserted through the ends of the housing. The main disadvantage with this design was that given the locations of the leaflets and hinges, the leaflets would open into the space above the housing which could be harmful to vessels or anatomical features above the housing. Backflow pressures would also create a large moment on the hinges and pins potentially leading to cyclic loading issues as a result of fatigue. These characteristics were taken into account and based on them and client feedback the sketch was redesigned.

3.1.2 Redesigned Sketch

Bottom View	Cross Section - Leaflet

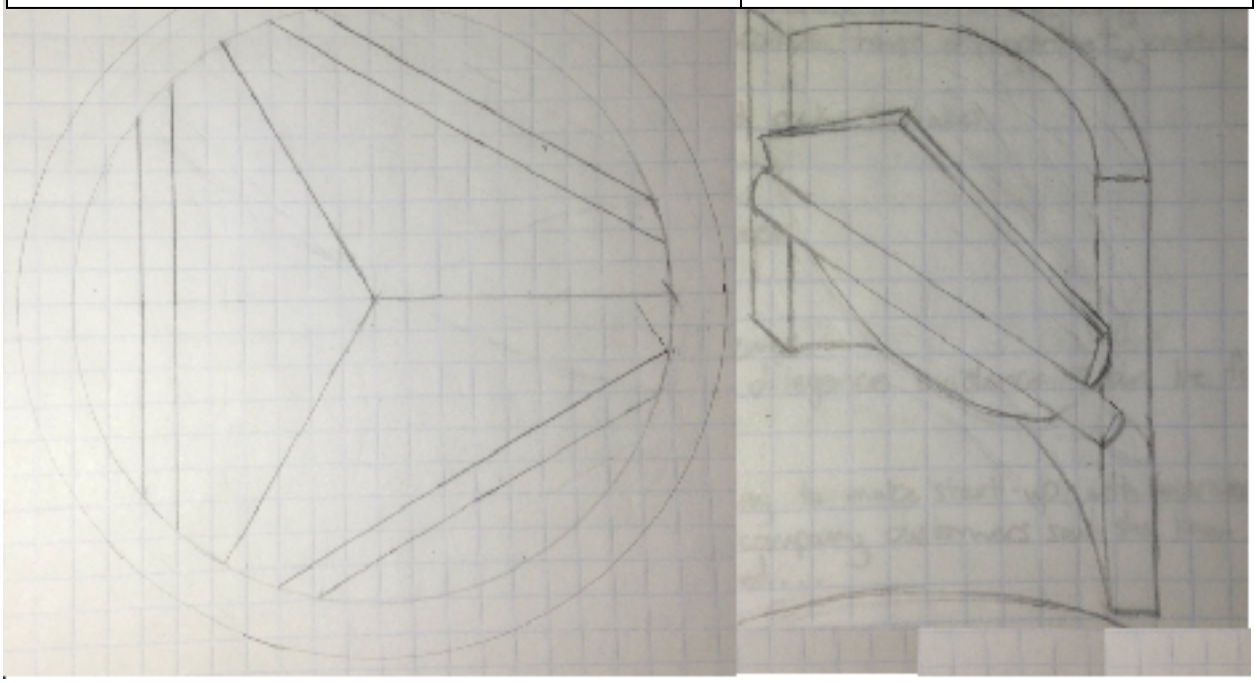

FIGURE 5: SKETCHES OF REDESIGNED TRI-LEAFLET DESIGN

The redesigned tri-leaflet valve contained the same number of components as the original design, but some modifications were made. The pins were moved from the edge of the housing towards the center in order to reduce forces acting on the pin when opening and closing. These forces were expected to be lower because a force applied to the leaflet would be more evenly distributed instead of creating a large moment like in the previous design. The leaflets were also moved down into the housing so that when opening and closing they are more contained and will not pose a risk to anatomical structures. A disadvantage associated with moving the leaflets into the housing is that cuts into the housing must be made in order to allow for a wider range of leaflet movement.

3.1.3 SolidWorks Model

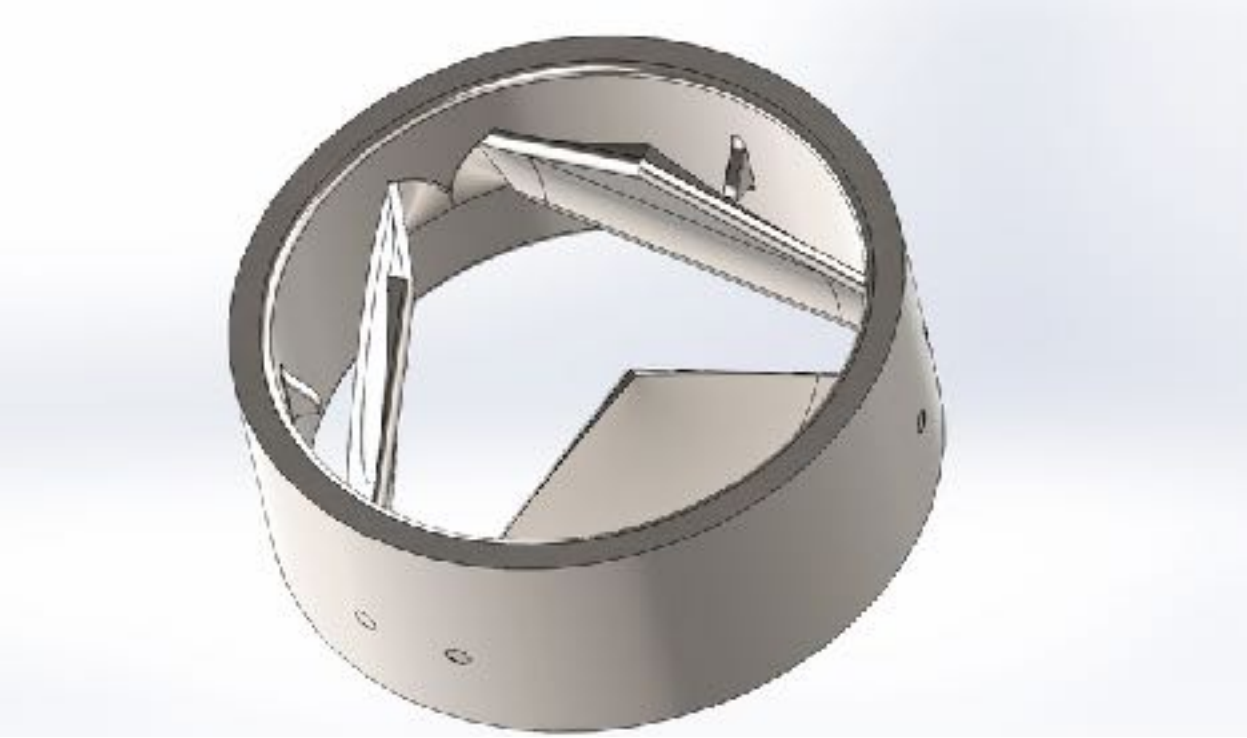

FIGURE 6: SOLIDWORKS MODEL OF TRI-LEAFLET DESIGN

Based on the feedback from the Interim report design modifications were made in order to satisfy functionality issues. The leaflets were given a curved face in order to assist in opening and closing the valve under flow conditions. The curvature on the top face of the leaflet extended from the center to the grooves in the housing with a peak where the center of flow would be located. This curvature was created in order to distribute pressure over the closed surface. Stoppers were also added to the housing to prevent the valve from over rotating when swinging closed and adding structural support to the leaflet when in the closed position. The bottom faces of the leaflets were filleted along the edging in order to focus flow on the space in between the leaflets to open the valve under lower pressures. In addition to the edging, the bottom portion of the leaflets that contain the pivot pin were also smoothed to encourage laminar flow around the leaflet. The grooves that were added to the design were shaped in order to form a flat connection with the top edge of the leaflet when in the open position. This contact acts to translate some of the flow forces into the housing of the design instead of only on the leaflet and pin. The SolidWorks model was also created as a 1:2 scale model in order to obtain success in printing an

ABS plastic model from the University of Guelph. The designed was scaled due to the limiting resolution of the printers, and some machining was required in order to obtain the intended functionality.

3.1.4 Redesign Based On Initial Testing

To implement the ABS printed valve in the Heart and Lung Simulator connecting pieces were designed to serve as adaptors from the valve to standard inch and a half male and female piping connectors. The designed connectors were seated inside the pipe connectors and surrounded most of the cylindrical housing leaving space for leaflet insertion. The adaptors however were unsuccessful for creating a water tight seal with the use of ABD cement and the design valve leaked during the experiment and some cement got into the housing causing the valve to be rendered useless. This problem was addressed by extending the housing and smoothing the edges associated with the increased diameter at the leaflet locations. The new housing was then cemented into the male and female adaptors as seen in the following figure.

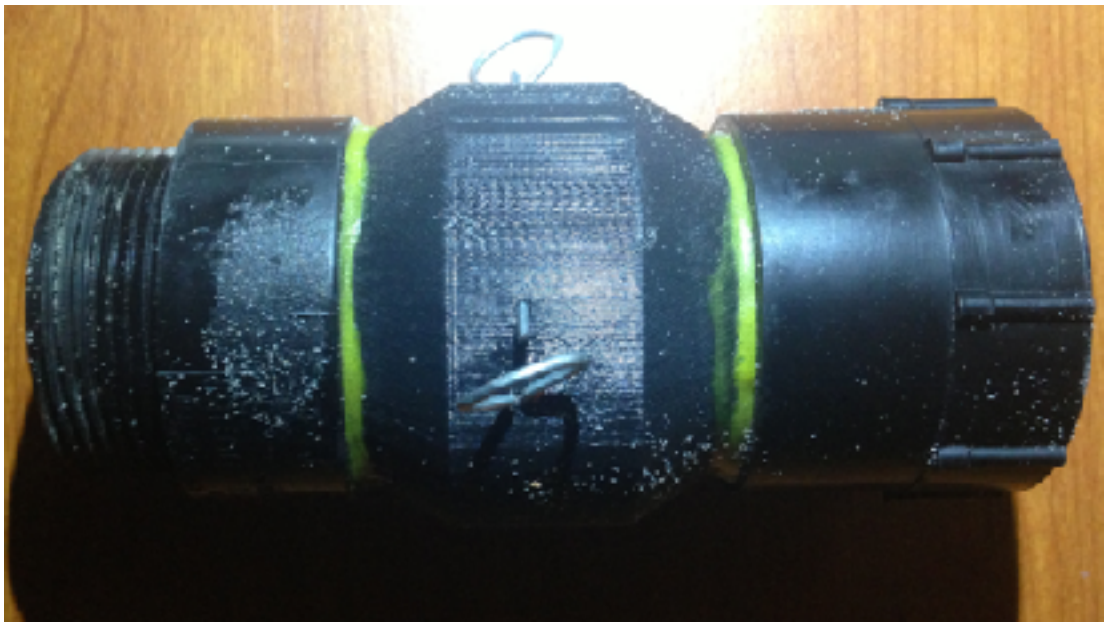

FIGURE 7: TRI-LEAFLET VALVE INSIDE EXPERIMENTAL APPARATUS

This experimental model contained very large spaced between the leaflets as a result of sanding to improve the functionality of the device. Sanding of the parts was necessary in order to eliminate the leaflet to housing connections which were a result of the lower printing resolution.

3.1.5 Final Model

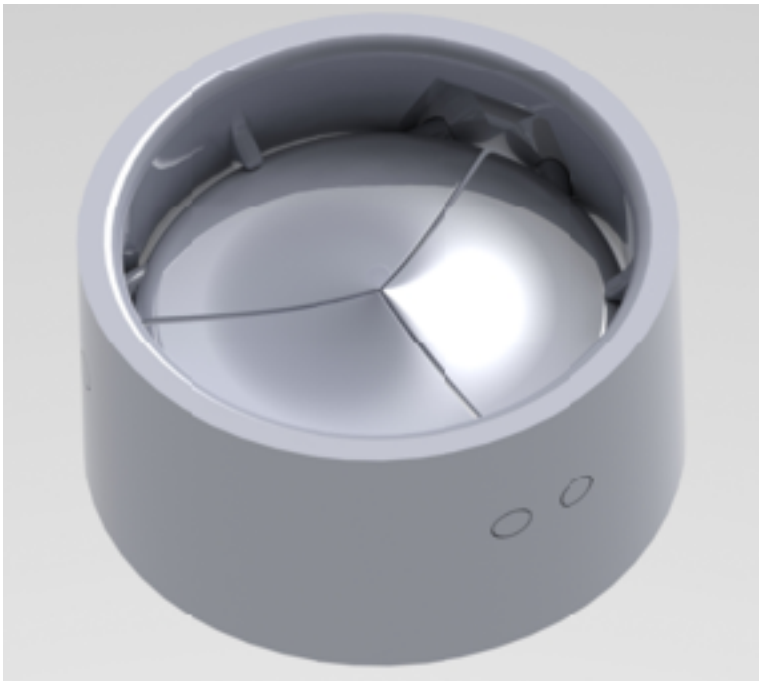

FIGURE 8: FINAL SOLIDWORKS MODEL OF TRI-LEAFLET DESIGN

Once the ABS model was successfully evaluated in the physical experiment and the computational methods were simulated, a final model was created to serve as the final prototype. A pin diameter of 2 mm was maintained from the up scaled model to increase the stress that the leaflet can withstand under physiological conditions. Another reason it was maintained was that the design will be less susceptible to fatigue caused by cyclic loading. The tolerances were also reduced to 0.1mm instead of the much larger tolerances used for the ABS model. The tolerances were required so that the design remains functional and depending on the accuracy of machining procedures, these tolerances may be reduced even more in future models. The grooves were also modified in order to eliminate the deep pits created by the corners of the leaflets when they swing into the open position. This was done in order to reduce the pooling of blood in these areas which can lead to red blood cell damage or coagulation.

3.2 Evaluation Process

3.2.1 Computational Fluid Dynamics

In order to examine the flow through the designed valves, a computational fluid dynamics (CFD) analysis was performed and compared against the flow characteristics of two existing mechanical heart valves. A 2-D analysis was performed due to the limiting licensure at the University of Guelph for the program Ansys Fluent which has a finite amount of memory available in each simulation. The analysis was designed to resemble the testing analysis performed in a study by Yin *et al*. who evaluated flow through the CarboMedics bileaflet and the Bjork-Shiley monoleaflet mechanical heart valves [43]. This study was selected because a 2-D analysis was performed on each valve to examine the flow velocities of blood as it passes over the leaflets which may cause damage to the platelets if blood velocities are too high, leading to coagulation on the valve. In order to perform a 2-D analysis in Fluent there are a number of steps which were completed consisting of: valve geometry setup, creation of a computational mesh, calculation parameters and solutions parameters, and the results of the analysis. These steps were completed for both designed valves and the bileaflet and monoleaflet valves evaluated in the journal article.

Valve Geometry

In order to obtain valve geometries in two dimensions, the valve designs were split in SolidWorks to obtain a cross section of the assembly. From there a 2D sketch was created on a parallel plane and copied to another SolidWorks part file. To ensure that the flow first contacting

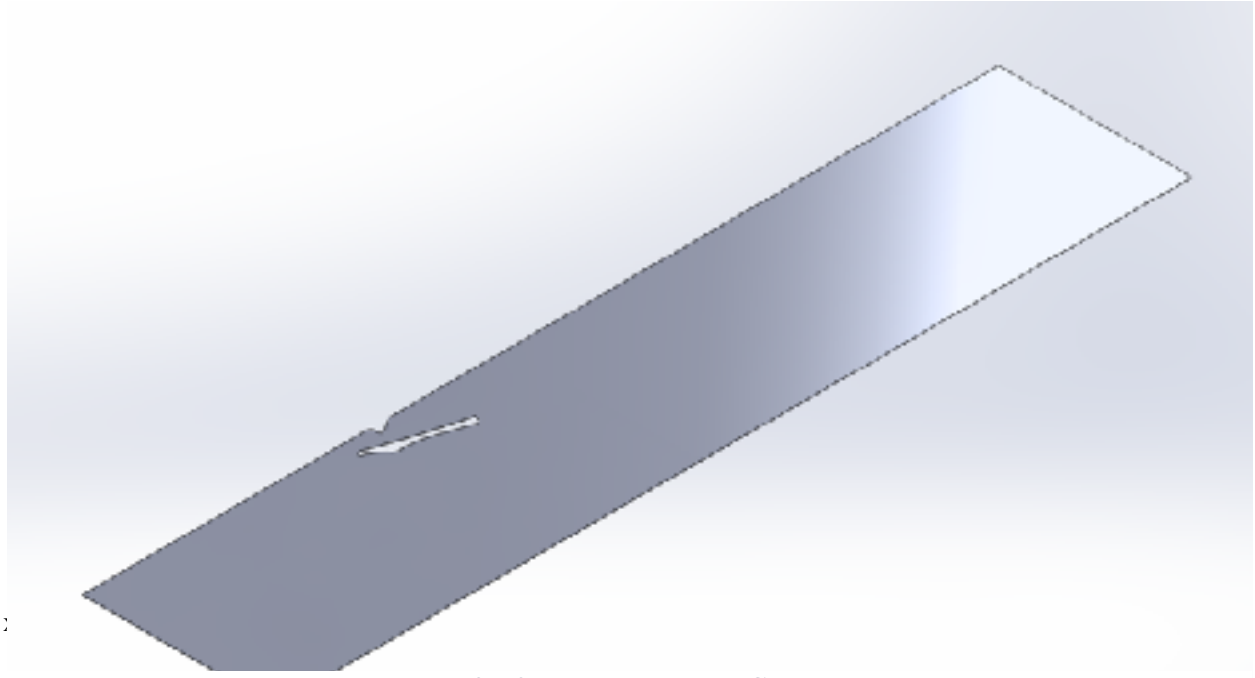

FIGURE 9 - 2D THIN WALLED GEOMETRY

the leaflet was uniform, the sketch housing containing the leaflet was extended in both inlet and outlet directions. The housing was extended in the outlet direction to 7 times the original length of the valve in order to observe the trailing flow patterns after travelling around the leaflet. The housing was extended 3 times in the inlet direction to ensure that the flow patterns are not irregular before reaching the leaflet geometry. The cross section sketch was then extruded into a 0.1mm thick plane which can be seen in the following figure.

Once the thin walled geometry was created, the file was saved in an .IGES format in order to be imported into Ansys Fluent. To obtain consistency between valve designs so flow velocities were comparable, the geometries were scaled to a housing diameter of 39.6mm. This diameter was obtained from a reference study [44] which contained the flow rates and valve diameters used in the Yin *et al.* CFD analysis.

The thin walled geometry was then imported into Fluent's fluid flow analysis system on the Fluent Workbench. A surface was created over the face of the thin walled geometry which serves as the computational surface for 2-D analysis in fluent.

Meshing

Once the geometry was imported and the surfaces were created, a mesh was required to set the number of computational nodes that were used to evaluate flow along the length of the 2-D geometry. The mesh was created in the mesh editor tool in fluent which opens the geometry to apply a mesh on the surface created earlier. A "Mapped Face Meshing" tool was applied to the surface of the geometry to specify the location of the mesh. In order to increase the number of computational nodes along target edges like around the leaflet and the walls of the cylindrical tube a sizing tool was used to select these edges. Once an edge was selected the number of mesh divisions along that edge may be specified depending on the size of the edge. For example the number of divisions used along the long edge of the geometry was 500 while the number of divisions along the leaflet was 50 due to the smaller length. After the number of divisions for each edge of interest was applied, the edges were labeled using Fluent's "Create Named Selection" tool which specifies the inlet and outlet of flow as well as the walls the fluid will flow around such as the leaflet. The number of computational nodes created in each mechanical heart

valve geometry ranged from 16,000 nodes to 20,000 nodes, however Yin *et al.* contained around 89,000 nodes. This difference occurs because in the article a 2-D aortic passageway was created to house the valves as opposed to the CFD that was performed in this project which utilized a long cylindrical tube in order to simplify the parameters to be compared. Another reason for this difference is the limiting available memory of Fluent when used through the University of Guelph's license. An image of the resultant mesh for the tri-leaflet design can be seen in the following image.

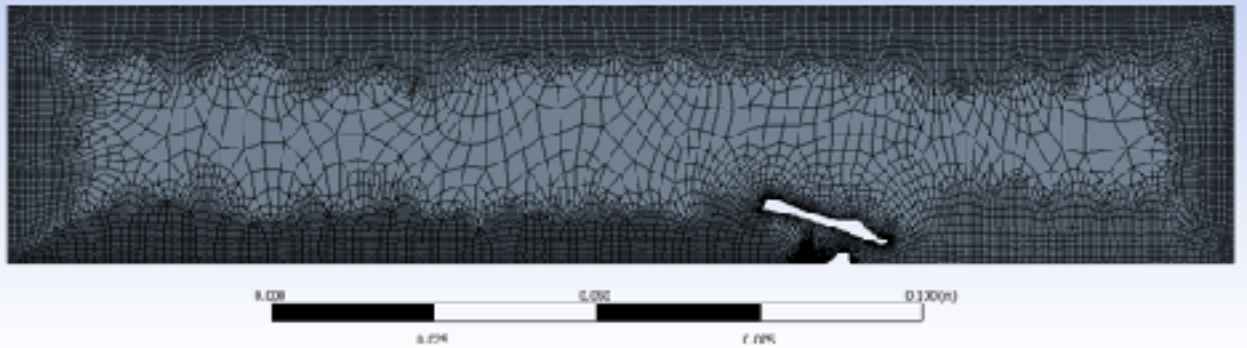

FIGURE 10 - MESH ON 2D GEOMETRY

Calculation and Solution Parameters

After the mesh was completed, parameters were required in order to ensure that Fluent calculated the desired fluid flow through the geometry. The setup was performed by opening the Fluent processor and first checking if the mesh was successful and determining the number of computational nodes that were created. It was also possible to check over the labeling of the specified walls such as if the inlet and outlet are located on the correct edges. The flow type was also specified as a standard k-omega with default parameters to match the flow type in Yin *et al.* Next, the material properties of the fluid were set by creating a new fluid model with the density and viscosity of blood whose values were obtained through [44]. The boundary conditions were set at the inlet and outlet, where the inlet velocity was calculated using the formula:

$$V = \frac{Q}{A} \quad and \quad A = \pi r^2$$

Where V is the inlet velocity, Q is the flow rate, and A is the cross sectional area of the valve opening, and ‘r’ is the radius of the valve diameter. The condition set at the pipe outlet was set to a zero pressure environment so there were no backflow forces.

The solution was set to evaluate as a second order upwind in the solution methods and was set to calculate the solution from the inlet. The convergence criteria were then set to 1e-6 in each Cartesian direction in order to obtain more accurate results while not taking much computing time. To achieve a more accurate simulation, the solution was run for 1000 iterations before determining the results. The results tab in Fluent was then opened to view the numerical and graphical solution and a flow vector was applied to get the resultant figure following.

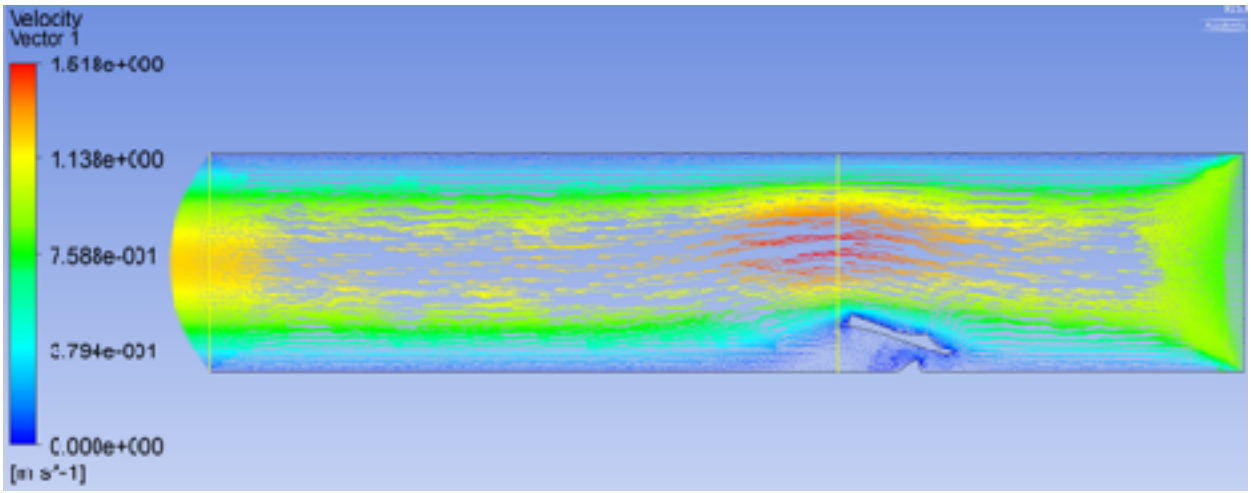

FIGURE 11 - VELOCITY PROFILE FOR TRI-LEAFLET DESIGN

From this graphical solution it is possible to calculate a localized Reynolds number from a velocity profile chosen with the wireframe line seen in the velocity profile above, intersecting the increased flow velocity. The Reynolds number was calculated according to the formula:

$$Re = \frac{v*P*2*r}{\mu}$$

Where v is the instantaneous flow velocity, P is the density of blood, r is the radius of the tube, and μ is the viscosity of blood.

3.2.2 Finite Element Analysis

A finite element analysis (FEA) was performed using SolidWorks 2014 simulation on both the tri-leaflet model and the tilting disc hinge model. The 3-D models were first assembled in SolidWorks and were given mechanical mates so the valves could open and close appropriately. The mates allowed the tri-leaflet valve open and close at an approximate 45 degree angle and allowed the tilting disc hinge valve to open and close at a 90 degree angle. The material that was selected was AISI type 316L stainless steel that was available in SolidWorks 2014 see appendix material properties *Table 17.* The boundary conditions were simplified by first setting up fixtures on the outside of the housing, inside the leaflet pin hole and the ends of the pins. This was done to simulate the exterior housing being attached to the body wall, and to simulate the pins rotating. Contact points were added between the struts of the housing and the leaflets, and between each leaflet. In order to determine the optimum mesh size that would ensure accuracy of results three meshes was created; a fine, course and normal mesh. All meshes had 4 Jacobian points. Total nodes of around 80000, 15000 and 3000 were used for the fine, normal and course mesh respectively for both valves. Pressure loads of 0.015998 MPa, which is equivalent to 120 mmHg was applied to the top of each leaflet and 0.009332 MPa which is equivalent to 70mm Hg was applied to the bottom of each leaflet. These values represent the systolic and diastolic pressures, see *Figures 12* and *13* for orientation of leaflets. The stress, strain, factor of safety and displacement were recorded and compared.

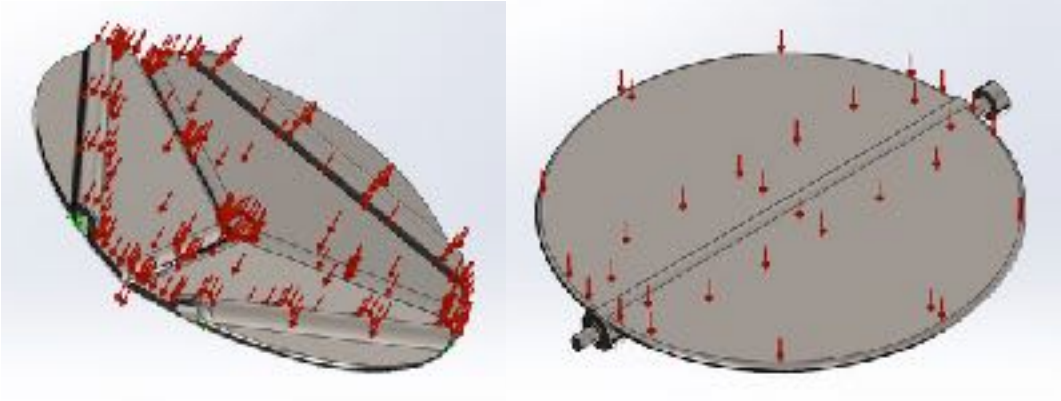

FIGURE 12: DIASTOLIC PRESSURES APPLIED AT THE BOTTOM OF BOTH LEAFLETS

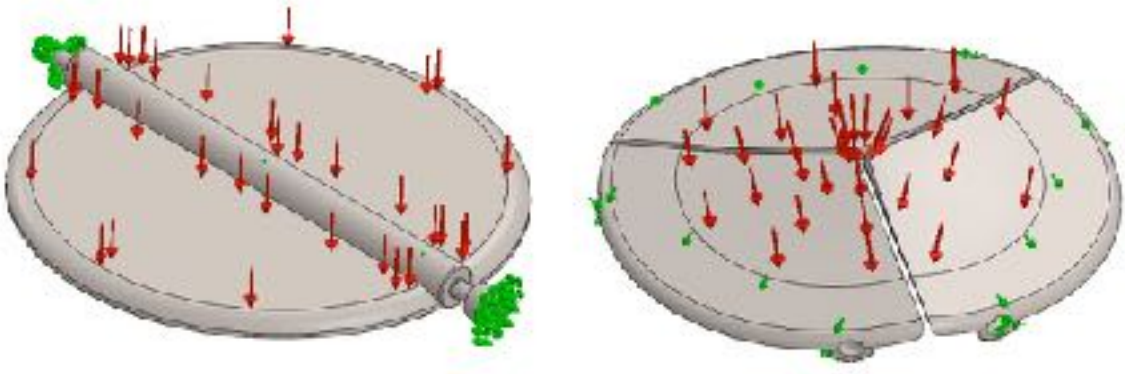

FIGURE 13: SYSTOLIC PRESSURES APPLIED AT THE TOP OF BOTH LEAFLETS

3.2.3 Experimental Testing

The use of an ex Vivo equine heart and lung simulator was provided by Dr. John Runciman and Dr. Bruce Guest. This system was originally a research tool that was designed and constructed for studies by *Guest, Arroyo, Viel, Kerr & Runciman*, (2014) to examine the hemodynamic and mechanical phenomena associated with the equine pulmonary vascular system [45]. A fresh heart and lung was collected from an adult horse and placed in normal anatomical position within a chamber. A closed loop, pulsatile, vascular circulation system was set up to simulate arteries and veins [45]. The system used a salt based solution which was drawn from a

larger reservoir and was heated to regular homeostatic body temperature, around 37 °C using heating coils [45]. An AC synchronous motor drew the solution up at a maximum flow rate of 120 L/min, which was adequate for resting conditions. An additional stepper motor and pulse valve were also used to replicate a pulse. The system then led to an instrument chamber which connected the perfusate from a pulse valve to the venae cavae and allowed for the entry of an endoscope and catheter to the heart, see *Figures 34 and 35*.

For the purposes of this project an actual horse heart and lung will not be used, rather a closed loop system will be designed around the heart and lung simulator to replicate an atrioventricular valve. *Figure 14* below shows the configuration of the experimental apparatus that was designed to simulate the flow across an atrioventricular valve.

FIGURE 14: EXPERIMENTAL APPARATUS USED IN THE HEART AND LUNG SIMULATOR

As seen from the figure, the apparatus is composed of an inlet, outlet and discharge valve. The designed heart valve was constructed in ABS plastic for this test. The valve was oriented so that ventricular side was facing the inlet and the atrial side was facing the outlet. A stepper motor was used to pulse water through the inlet simulating the systolic pressure of the valve. Any leakage from the valve will fill the outlet hose. The amount of leakage was approximate due to some leakage through the pins of the housing. The discharge valve and the water in the outlet hose were then used to simulate diastolic pressure. An endoscope was sent through the

tubing to monitor valve functionality and flow across the valve. The measurements that were taken from this experiment were as follows:

1. The diastolic and systolic pressures were read from a pressure gage
2. The amount of water pumped by the AC motor was measured by a flow gauge
3. The amount of leakage was measured in the outlet tube.
4. The opening diameter was observed through the endoscope.

The average velocity across the valve, the Reynolds number and the mass flow rate can be determined using the conservation of mass and Poiseuille's relationship. The following assumptions need to be made for these values to be calculated:

- laminar flow
- steady flow
- use of a Newtonian fluid

It should be noted that even though laminar flow is assumed it will later be verified in the calculations. The following equations were used to calculate the average velocity and Reynold's number. *These equations were obtained from [46].

Poiseuille's Relationship

1. Determine the average velocity across the valve.

$$v_{avg} = \frac{Q}{\pi r^2}$$

   Where v_{avg} is the average velocity, Q is the flow rate and r is the radius.

2. Determine the change in HGL. (Note: since the outlet tube was held at an angle of approximately 180 degrees z = L)

$$Q = \frac{\pi \rho g d^4 h_f}{128 \mu L}$$

$$h_f = \frac{128 \mu L Q}{\pi \rho g d^4}$$

Where h_f is the headloss, μ is the dynamic viscosity, ρ is the density, g is the acceleration due to gravity, L is the length of the outlet tube and d is the diameter.

3. Determine the Reynold's number.

$$Re = \frac{v_{avg} d}{\nu}$$

Where Re is the Reynold's number and ν is the kinematic viscosity.

Conservation of Mass

4. Determine the mass flow rate across the valve.

$$mass flow rate = \rho_1 A_1 V_1 = \rho_2 A_2 V_2$$

Sample calculations and an analysis of the results can be found in *A.1: Detailed Design Calculations* and *Section 4.1.1 Physical Design*.

3.4.4. Decision Making Tools

TABLE 10: DECISION MATRIX COMPARING THE TRI-LEAFLET DESIGN AGAINST THE TILTING DISC VALVE DESIGN

	Characteristics	Experimental Values		Score /10		Weighting /1	Weighted Score		
		Tri-leaflet	Tilting Disc	Tri-leaflet	Tilting Disc		Tri-leaflet	Tilting Disc	
Physical Testing	Pressure to Open/Close (Diastolic/ Systolic)	26.18/ 86.02	>26.18/8 6.02	9	2	0.25	2.25	0.5	
	Surface Area of Open Valve (mm^2)	1735	1294.19	8	5	0.08	0.64	0.4	
Finite Element Analysis (Systolic)	Displacement (mm)	0.0022	0.00119	7	8	0.1	0.7	0.8	
	Strain	1.00E-05	1.05E-05	7	8	0.16	1.12	1.28	
	Stress (N/m^2)	3.58E +06	3.21E+06	8	6	0.16	1.28	0.96	
Computational Fluid Analysis	Flow Velocity (m/ s)	1.52	1.74	8	6	0.25	2	1.5	
						1	7.99	5.44	Total

Quantitative results were used for the weight of each design for the decision matrix. For physical testing both the pressure and surface area was analyzed. The tri-leaflet valve had a pressure to open/close of 26.18/86.02. These pressures represented the Diastolic and Systolic pressures. Since the tilting disc valve did not open during testing it was given an experimental value of greater than 26.18/86.02 and much lower score. This was one of the main areas that was focused on for physical testing this section was given a large rating of 0.25. The surface area of the valves open was not as significantly weighted as the discussion on the physical testing focused on flow and pressure. For the FEA only peak systolic values were chosen. Stress, strain and displacement were chosen as they were all affected by pressure. The stress and strain were given equal weighting as they were of primarily interest in the FEA discussion as it focused on the reaction to the pressures that would be applied on the valve. The displacement was given a lower weighting as was not the primary focus of the FEA discussion. Finally for the CFD analysis focused on flow velocity. This section was given a high rating because at high enough velocities platelet activation can occur and this could cause damage of the blood cells.

4.0 Results and Discussion of Selected Design

4.1 Final Design

4.1.1 Physical Design

Out of the four heart valves, the aortic, tricuspid, and pulmonary valves are composed of three leaflets with supporting structures such as chordae tendinae. Therefore it is believed that

FIGURE 15 - HOUSING OF TRI-LEAFLET DESIGN

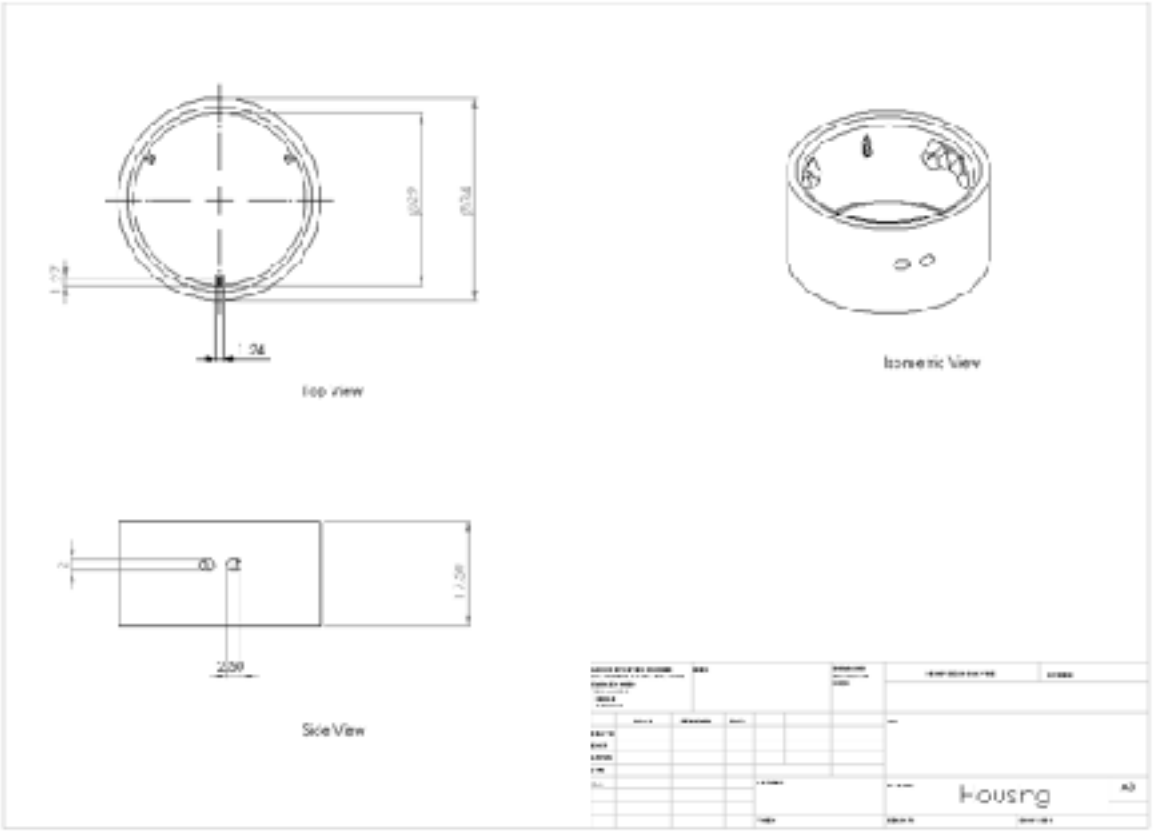

this tri-leaflet design would best imitate the natural functions of the valves from both an anatomical and physiological perspective. Two dimensional schematic drawings of the valve components can be seen in the following figures.

The design consists of a cylindrical housing, three leaflets or plates, and hinge pins inserted through the cylindrical housing and the leaflets to form a pivot point. In order to prevent the leaflets from contacting one another when opening, the edges of the plates are curved inward along the edges so that a complete seal is created between leaflets. This curving also created a flow concentration along the edges of the leaflets resulting in leaflet movement under lower flow conditions than the sharp edged model. Similarly the edges of the leaflets that come into contact with the cylindrical housing are also curved so they do not become restricted on the housing wall when they rotate downwards. Another concern that was addressed is the potential contact with

FIGURE 16: LEAFLET DESIGN OF TRI-LEAFLET VALVE

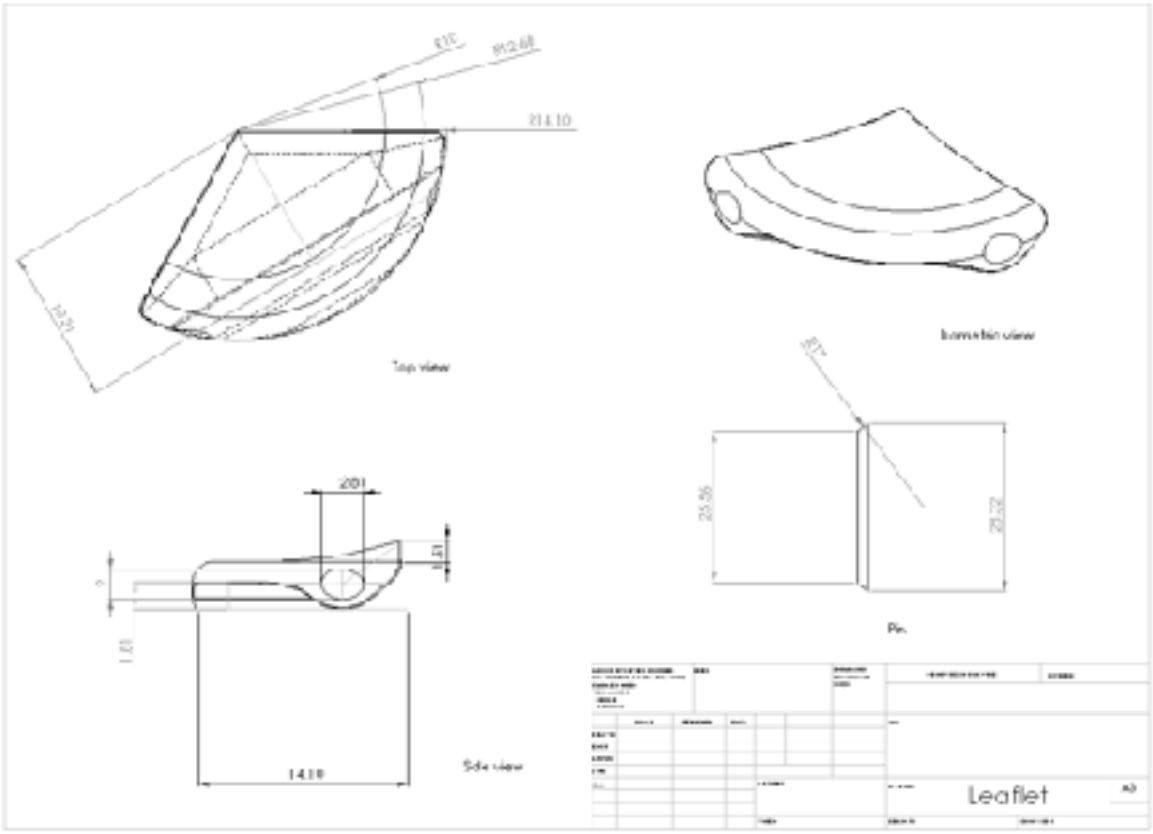

the wall of the vessel when the leaflets are in the open position. This has been solved by placing a stop on the housing so that their range of motion will be limited and contained within the housing. These stops are in the form grooves cut into the housing in order to allow for a wider range of leaflet movement. Additional stops were added to the wall of the housing in order to catch the leaflet in the closed position to prevent the leaflet from over turning and extending in the opposite direction. The stops added to the housing were smoothed to reduce the amount of turbulence caused by the extrusion into the flow space. The design was contained within the cylindrical housing with exception to the tips of the leaflets which extend above the top of the housing when in the open position. This small extension above the housing exit is not significant enough to make contact with vessels or structures within the heart. All edges have been rounded to ensure that blood flowing over the edges is not damaged by concentrated turbulence.

The greatest difference when compared to existing designs is the tri-leaflets, which may mimic natural physiology better than the alternative solutions and will have less loading stresses on each pin because the leaflet weights are distributed across three pins opposed to one or two.

There are also two mechanisms for stopping a leaflet once it has achieved its open and close positions, where the other mono-leaflet design has one for each moving component.

4.1.2 Computational Fluid Dynamics Analysis

As mentioned in design methodology, a computational fluid dynamic analysis was performed on the tri-leaflet and mono-leaflet designs as well as the CarboMedics bi-leaflet and the Bjork-Shiley mono-leaflet mechanical heart valves. The resultant velocity profiles as well as velocity magnitude profiles for both valve designs as well as the Bjork-Sheiley mono-leaflet and CarboMedics bi-leaflet valves can be seen in the following figures.

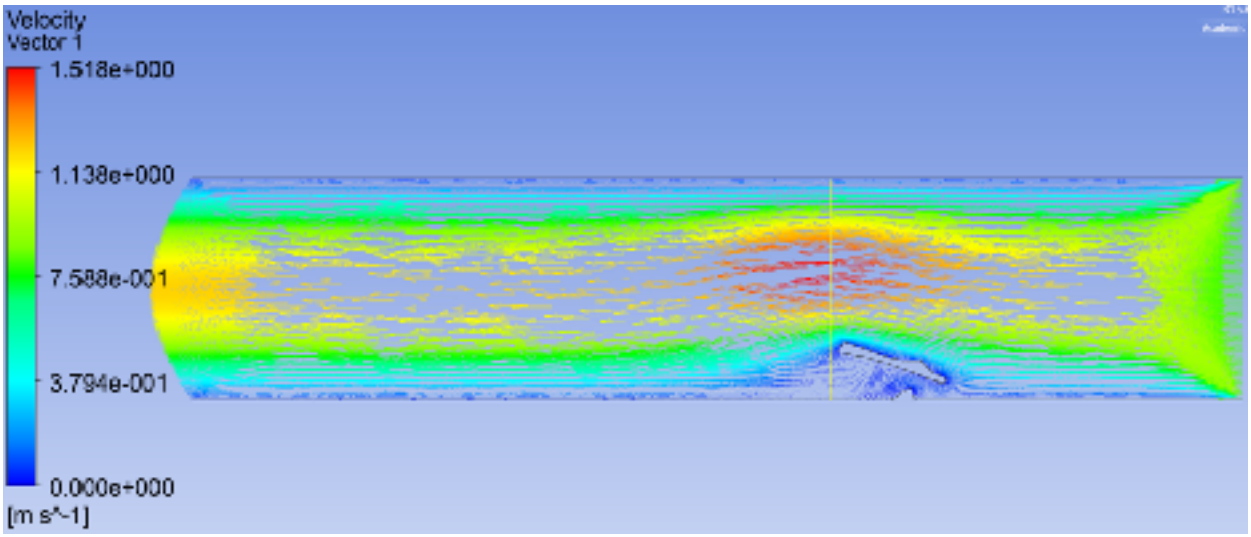

FIGURE 17: VELOCITY CONTOUR FOR TRI-LEAFLET VALVE

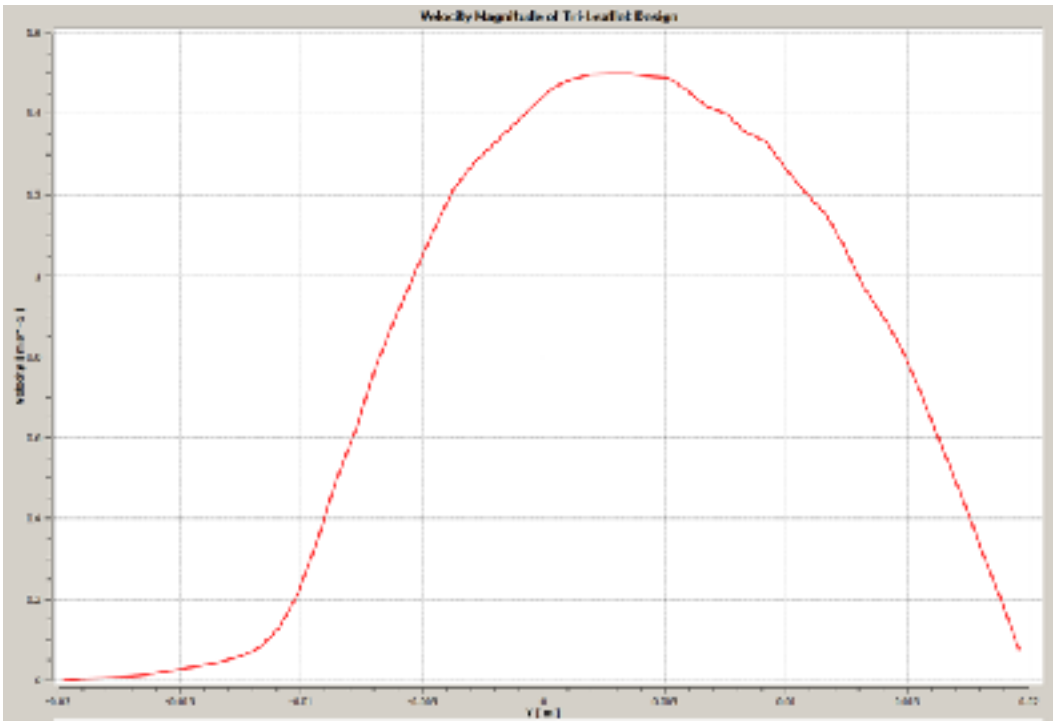

FIGURE 18: VELOCITY MAGNITUDE FOR TRI-LEAFLET VALVE

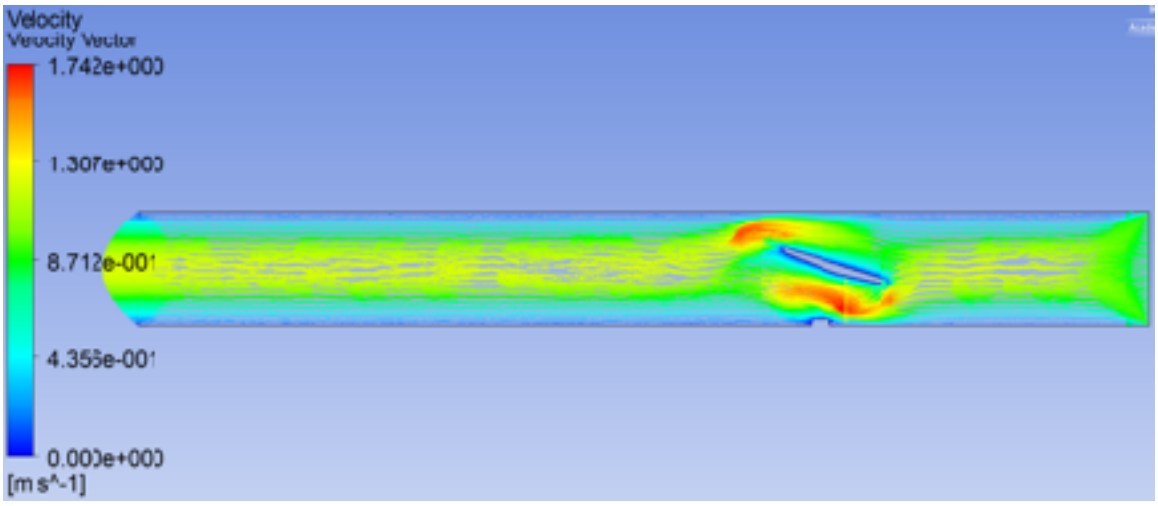

FIGURE 19: VELOCITY CONTOUR FOR MONO-LEAFLET VALVE

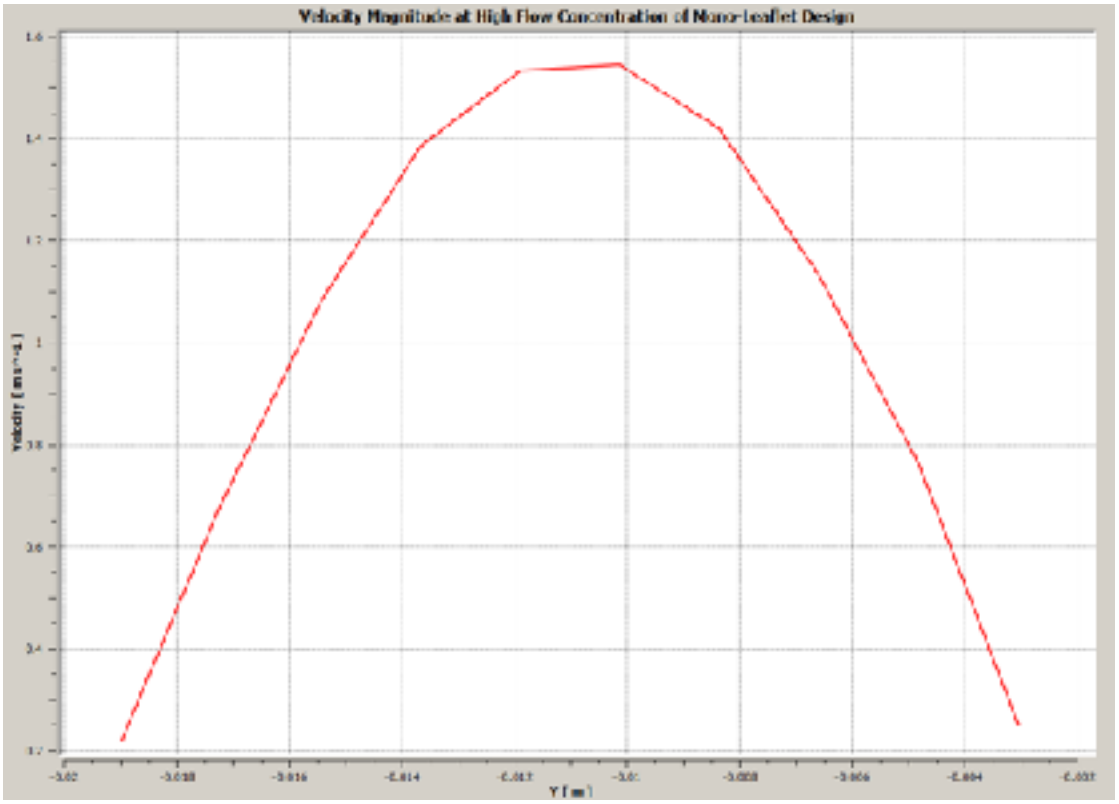

FIGURE 20: VELOCITY MAGNITUDE FOR MONO-LEAFLET VALVE

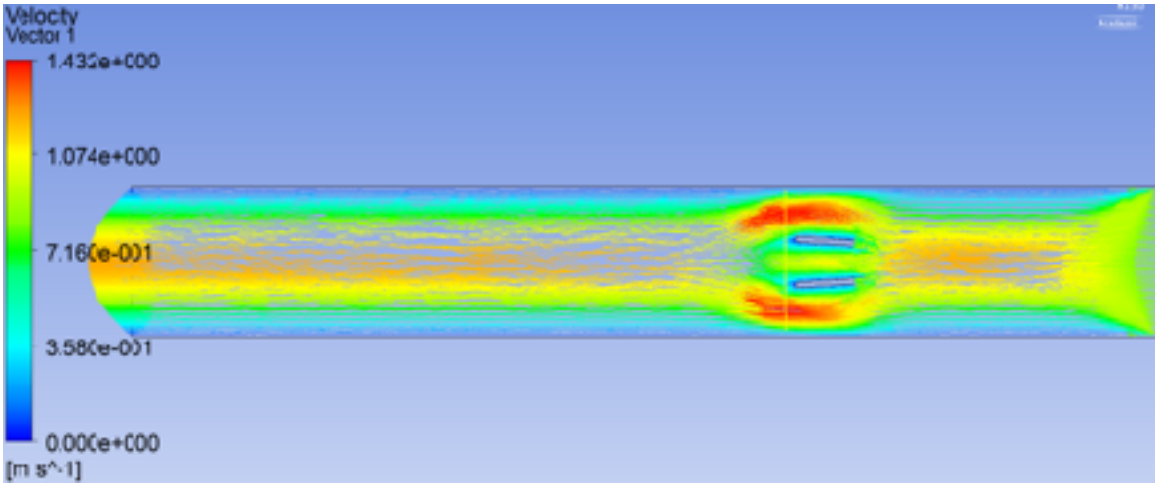

FIGURE 21: VELOCITY CONTOUR FOR CARBOMEDICS BI-LEAFLET VALVE

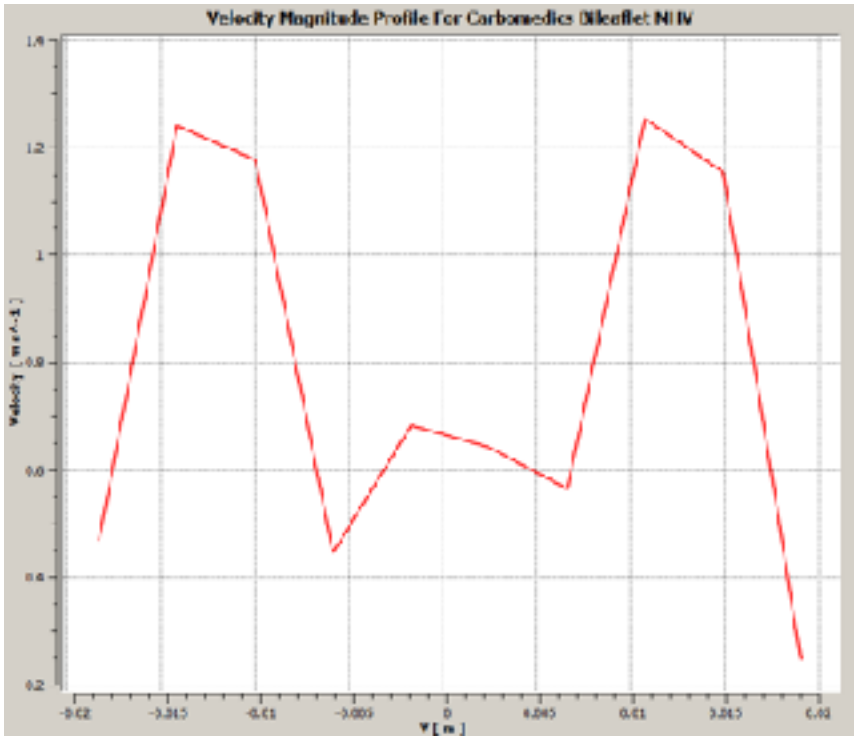

FIGURE 22: VELOCITY MAGNITUDE FOR CARBOMEDICS BI-LEAFLET VALVE

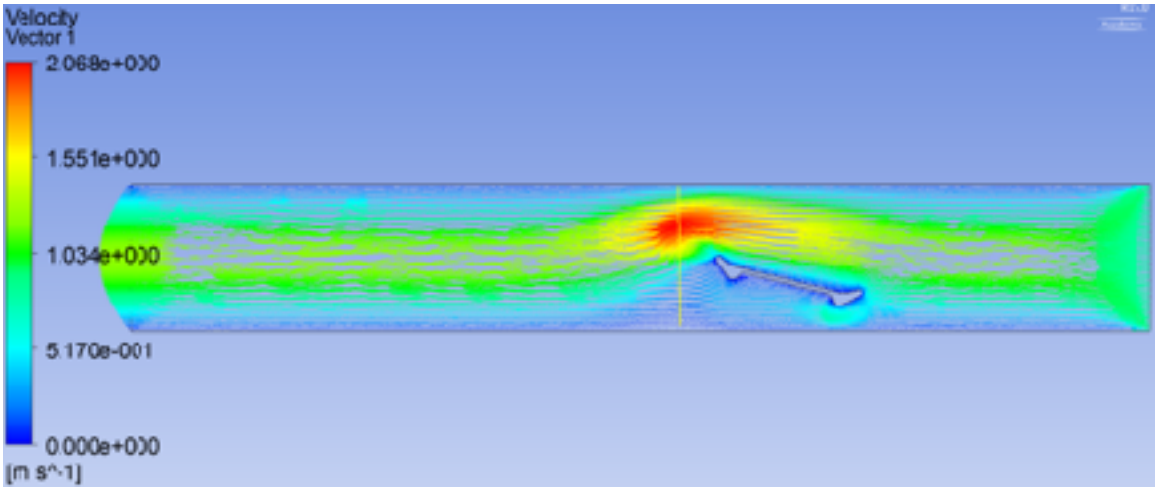

FIGURE 23: VELOCITY CONTOUR OF BJORK-SHILEY MONO-LEAFLET VALVE

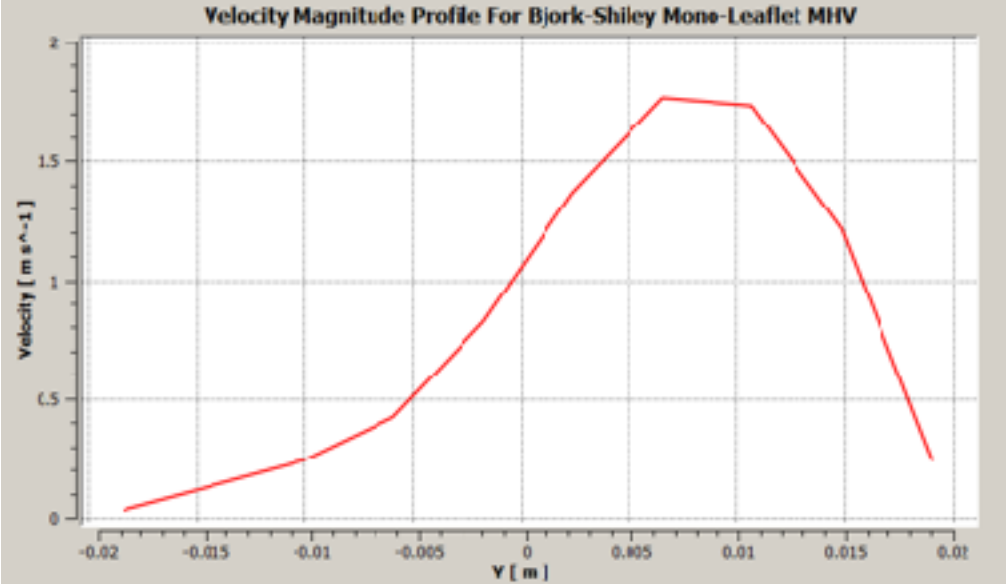

FIGURE 24: VELOCITY MAGNITUDE FOR BJORK-SHILEY MONO-LEAFLET VALVE

The maximum velocities in the models are as follows: tri-leaflet design contained a maximum velocity of 152 cm/s, the tilting disc design contained a maximum velocity of 174cm/s, the CarboMedics bi-leaflet valve contained a maximum velocity of 143 cm/s, and the Bjork-Shiley mono-leaflet valve had a maximum velocity of 207 cm/s. These results are comparable to the study conducted by Yin *et al.* who resulted in velocities of 134 cm/s and 167cm/s for the bi-leaflet and mono-leaflet valves respectively. The main cause of the difference in results is the experimental geometries. Yin *et al.* used an anatomical model for the aortic cross section, while the CFD performed for this project used a straight cylinder. This also has an effect on the flow patterns pictured above, however the same parameters were applied to the CarboMedics and the Bjork-Shiley valves in order to ensure experimental consistency. The inlet velocity for all of the above valves was calculated to be 0.812m/s using flow rate and vessel diameter from Bluestein *et al.* The calculated is also consistent with measured aortic velocities during rest using ultrasonic Doppler imaging [47].

Tri-Leaflet Design Discussion

The Reynolds number was calculated for the tri-leaflet design according to the formula:

$$Re = \frac{v*d*P}{\mu} = \frac{1.52\frac{m}{s}*0.0396m*1.2\frac{kg}{m^3}}{0.004(\frac{kg}{m*s})} = 18$$

Where v is the maximum velocity, d is the vessel diameter, P is the density of blood, and μ is the viscosity of blood. With such a small Reynolds number the flow through the tube should be laminar, however there is observed turbulence on the tri-leaflet design around the trailing edge of the leaflet (Refer to *Figure 17*). This is likely caused by the decrease in flow area between the leaflet and the stopper followed by an increase in flow area causing a low pressure region where flow velocity is extremely slow. The increased flow on the other side of the leaflet expands into this space once the blood has travelled past the leaflet causing the turbulent pattern in the velocity contour for the tri-leaflet design figure above. A recommendation for improving this would be to increase the range of motion of the leaflet so that the flow is less obstructed and the flow does not concentrate to one side of the leaflet. Additionally, the stopper can be made smaller or be designed with a better flow profile to eliminate the restriction it causes on the blood flow.

Turbulence is major factor to consider when designing a mechanical heart valve because excessive eddies in the flow apply shear forces to the blood which is associated with platelet activation and coagulation. Turbulence can be avoided by constricting the flow as little as possible by allowing a wider range of motion for the leaflets as well as consistent tubular diameter. The tri-leaflet design performs well under physiological flow velocities and with some adjustments to the leaflet ranges, the design forms a successful alternative to the CarboMedics and Bjork-Shiley mechanical designs.

4.1.3 Finite Element Analysis

A main advantage in conducting finite element analysis simulations is that it yields information on some characteristics of the heart valve, such as strains and stresses in the tissue, which are very difficult to determine experimentally. In this study, the stress-strain state of the valve at key points at peak systolic and diastolic pressures were investigated. During peak systolic pressures the maximum stresses and strains were found to occur at the middle of the

leaflet when the pin goes through the valve and going into to center for the tri-leaflet valve and spreading outwards for the tilting disc valve. A maximum stress of 3 211 kN/m^2 and 289.556 kN/m^2 was exerted on these areas for the tilting disc and the tri-leaflet valve respectively; where *Figures 25* and *26* show this in a normal mesh. The strains follow a similar trend as these same areas experience the most strains. Maximum strains of 1.053e-005 and 9.204e-007 was exerted on the tilting disc and tri-leaflet respectively; where *Figures 27* and *28* show this in a normal mesh. During peak Diastolic pressure the maximum stresses were found to occur at the middle of the leaflet when the pin goes through the valve. A maximum stress of 3 211 kN/m^2 and 2 453 kN/m^2 were exerted on these areas for the tilting disc and the tri-leaflet valve respectively; where *Figures 29* and *30* show this in a normal mesh. The strains follow a similar trend as these same areas experience the most strains. Maximum strains of 7.565e-006 and 7.152e-006 were exerted on the tilting disc and tri-leaflet respectively; where *Figures 31* and *32* show this in a normal mesh. In terms of the leaflet displacement both leaflets showed very little change. The tri-leaflet and the tilting disc valves had a maximum average displacement of 0.00220204 mm and 0.00119372 mm respectively; where *Figures 33* and *34* show this in a normal mesh.

When comparing both valves using FEA both valves yield similar results but the tri-leaflet valve yields better results. The tri-leaflet valve has a higher and more distributed stress and strain concentration along its leaflets. This means it can withstand a greater stress and strain and is likely because having multiple leaflets allows for the distribution of the loads and it allows for the leaflets to open up more easily. Once open the leaflets have a different pressures being applied on different location and it creates cyclic loading as the valves open and close. This opening and closing creates an even greater force distribution and does not allow for too much force to be applied on a single area for too long.

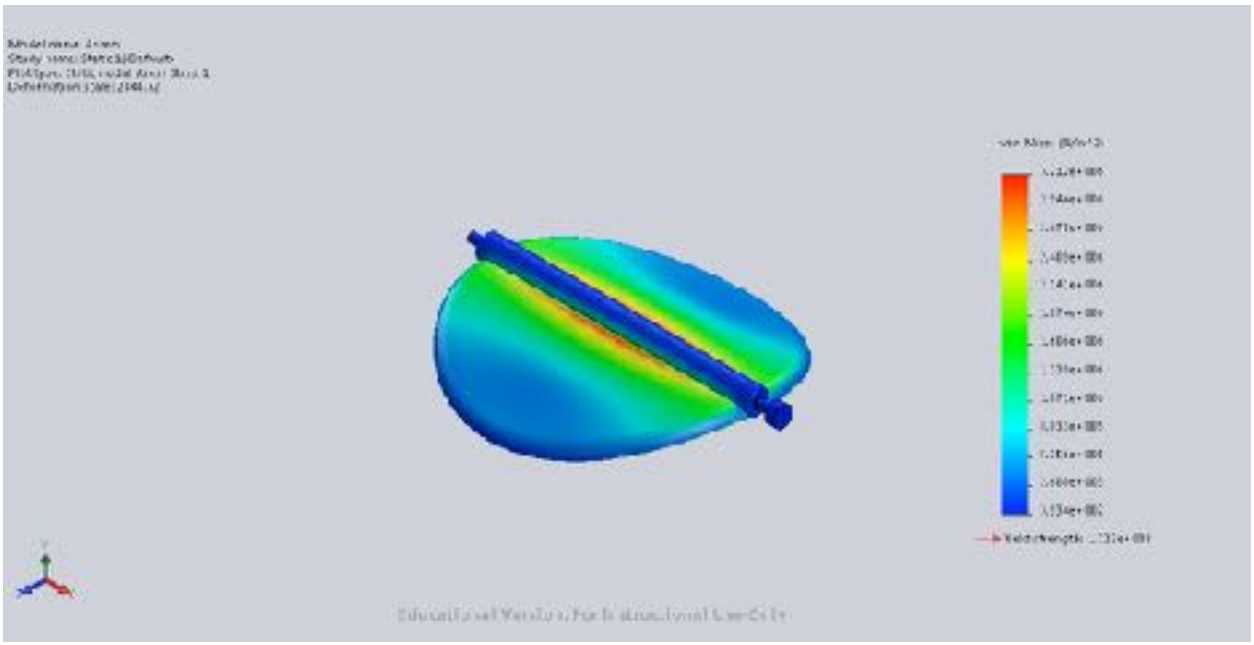

FIGURE 25: SYSTOLIC PRESSURE STRESS ALONG TILTING DISC VALVE WITH NORMAL MESH

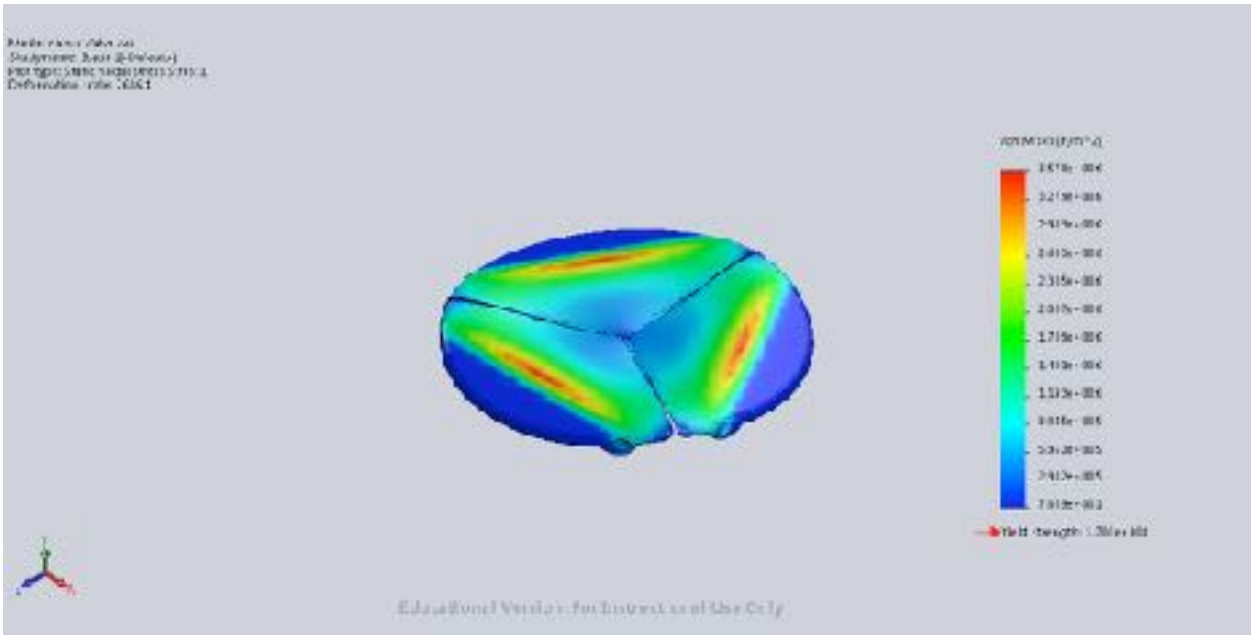

FIGURE 26: SYSTOLIC PRESSURE STRESS ALONG TRI-LEAFLET VALVE WITH NORMAL MESH

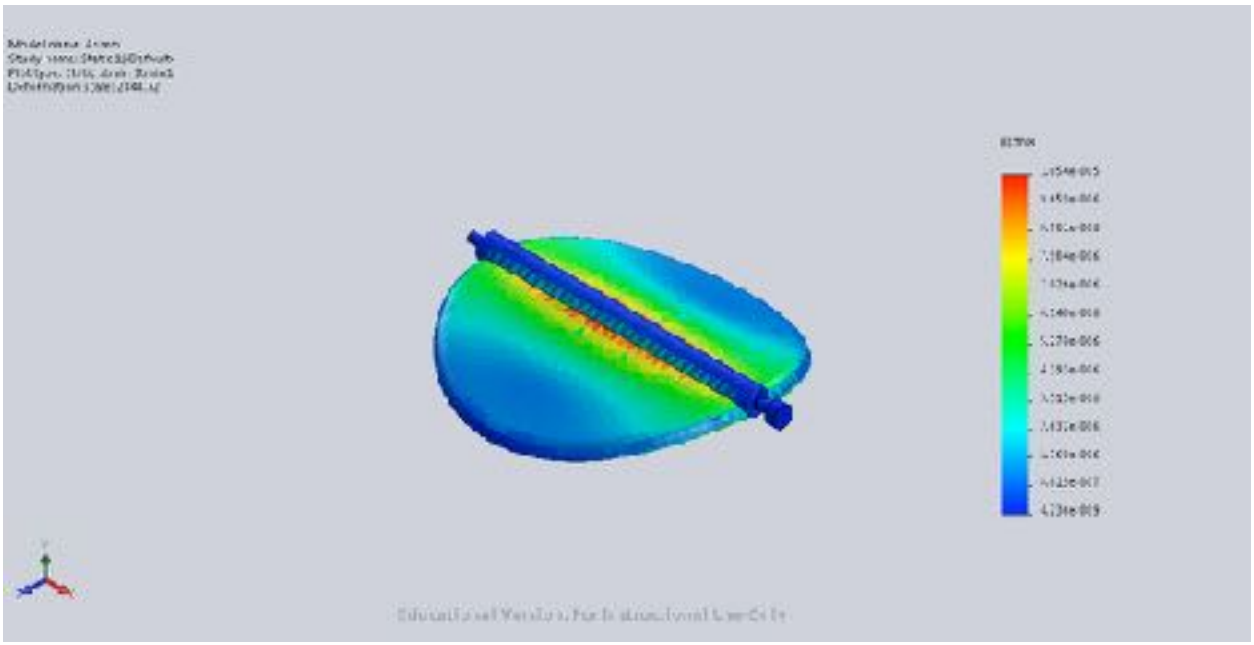

FIGURE 27: SYSTOLIC PRESSURE STRAIN ALONG TILTING DISC VALVE

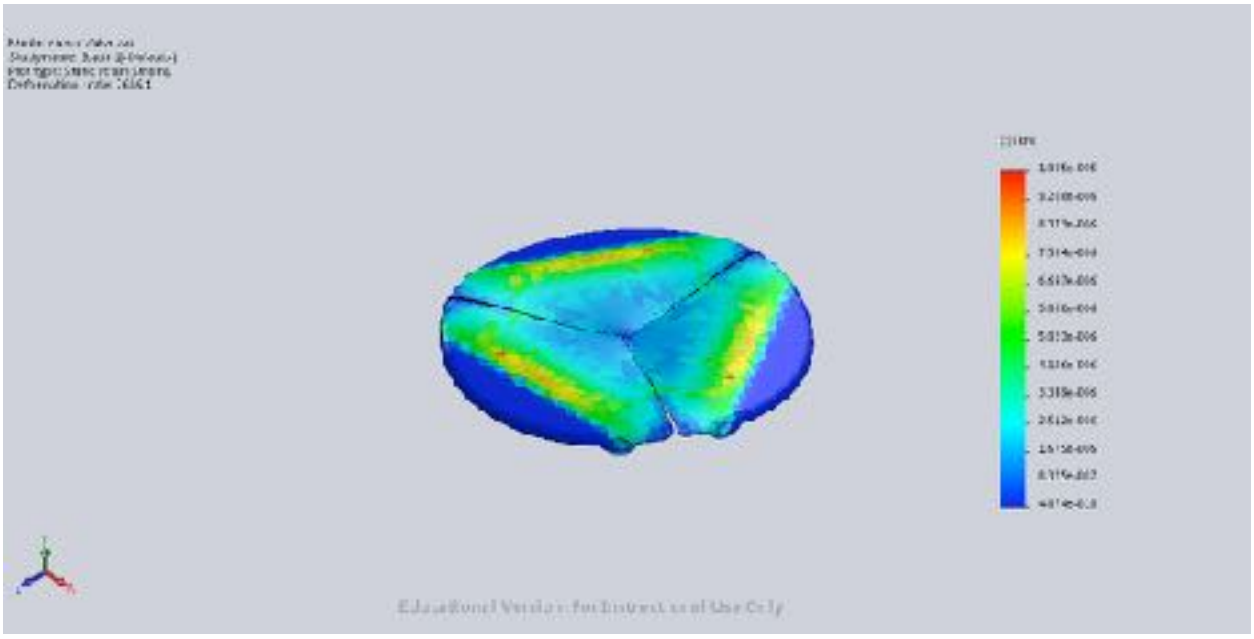

FIGURE 28: SYSTOLIC PRESSURE STRAIN ALONG TRI-LEAFLET VALVE

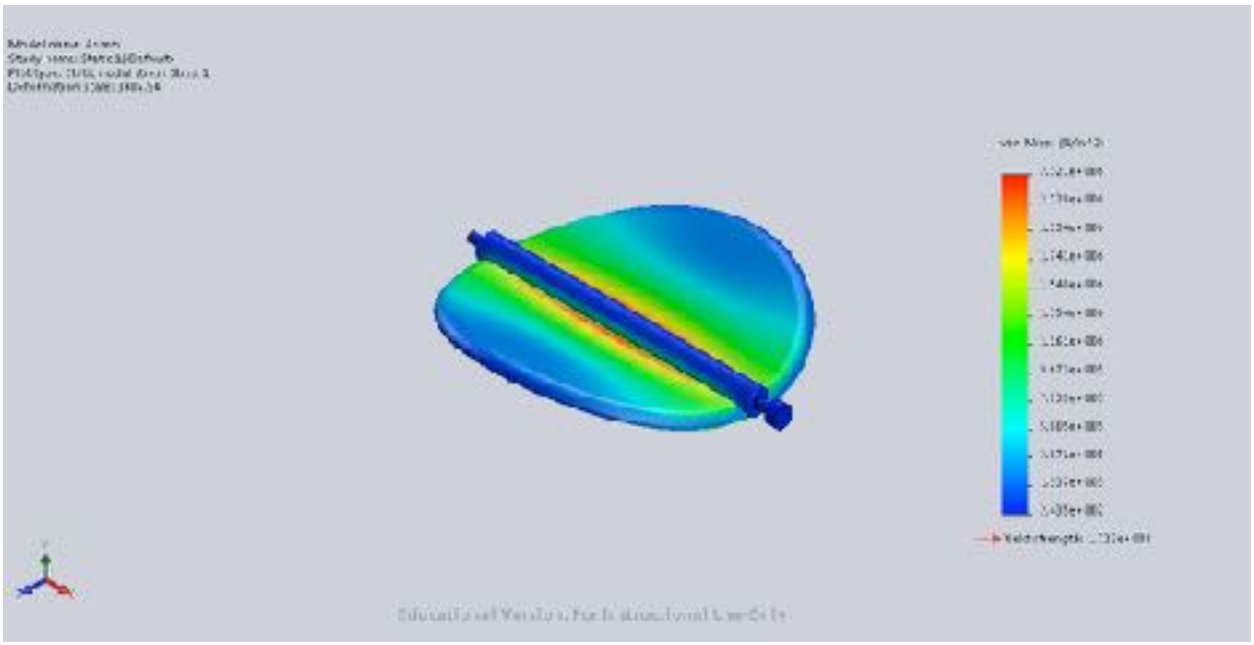

FIGURE 29: DIASTOLIC PRESSURE STRESS ALONG TILTING DISC VALVE

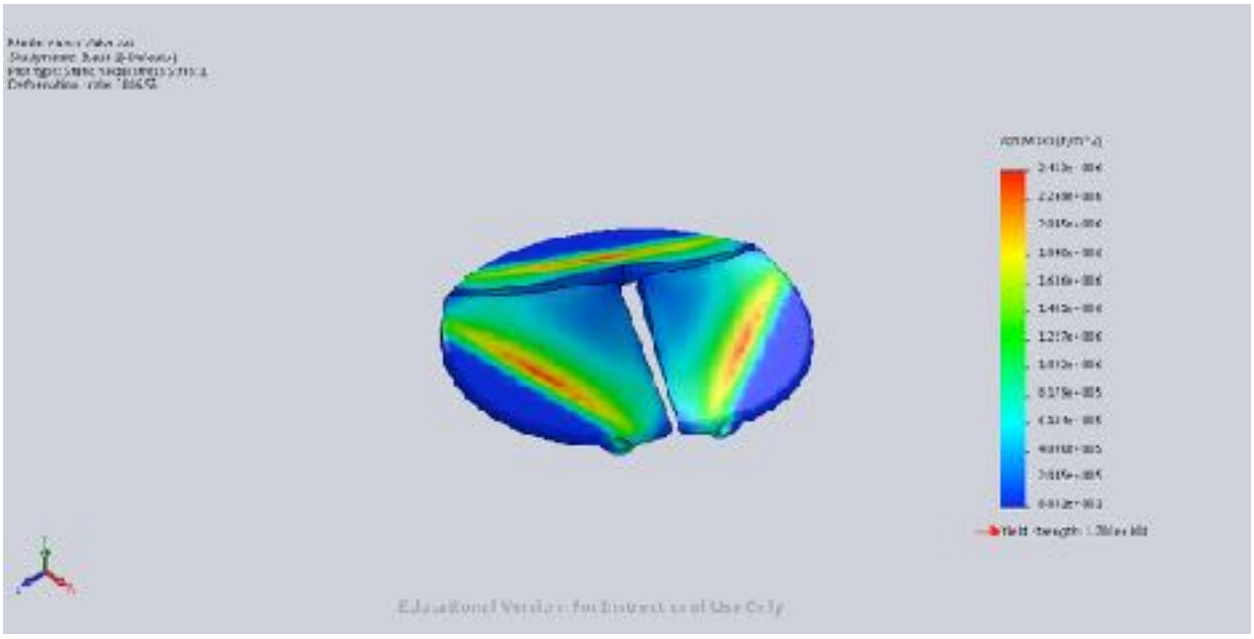

FIGURE 30: DIASTOLIC PRESSURE STRESS ALONG TRI-LEAFLET VALVE

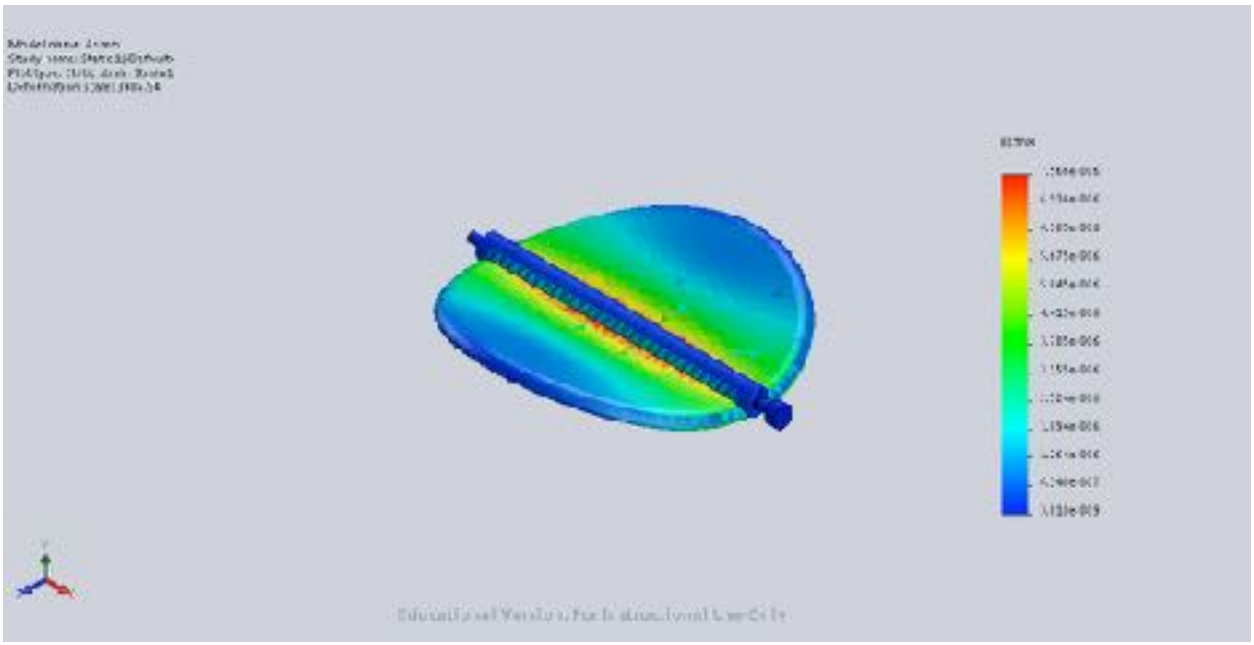

FIGURE 31: DIASTOLIC PRESSURE STRAIN ALONG TILTING DISC VALVE

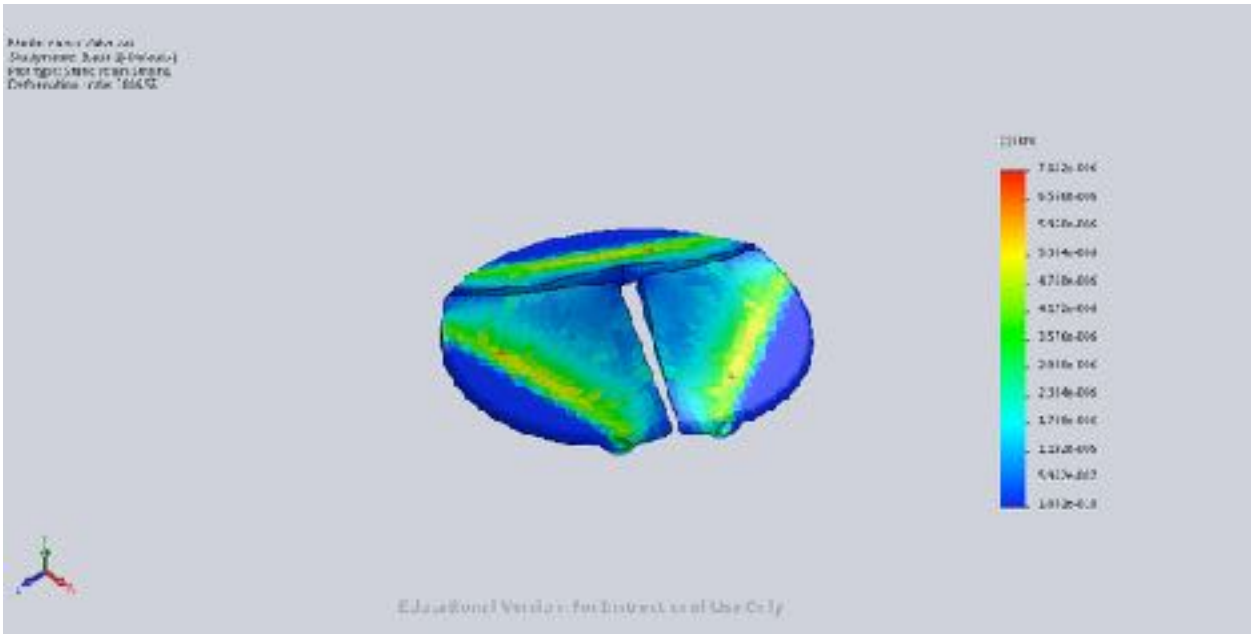

FIGURE 32: DIASTOLIC PRESSURE STRAIN ALONG TRI-LEAFLET VALVE

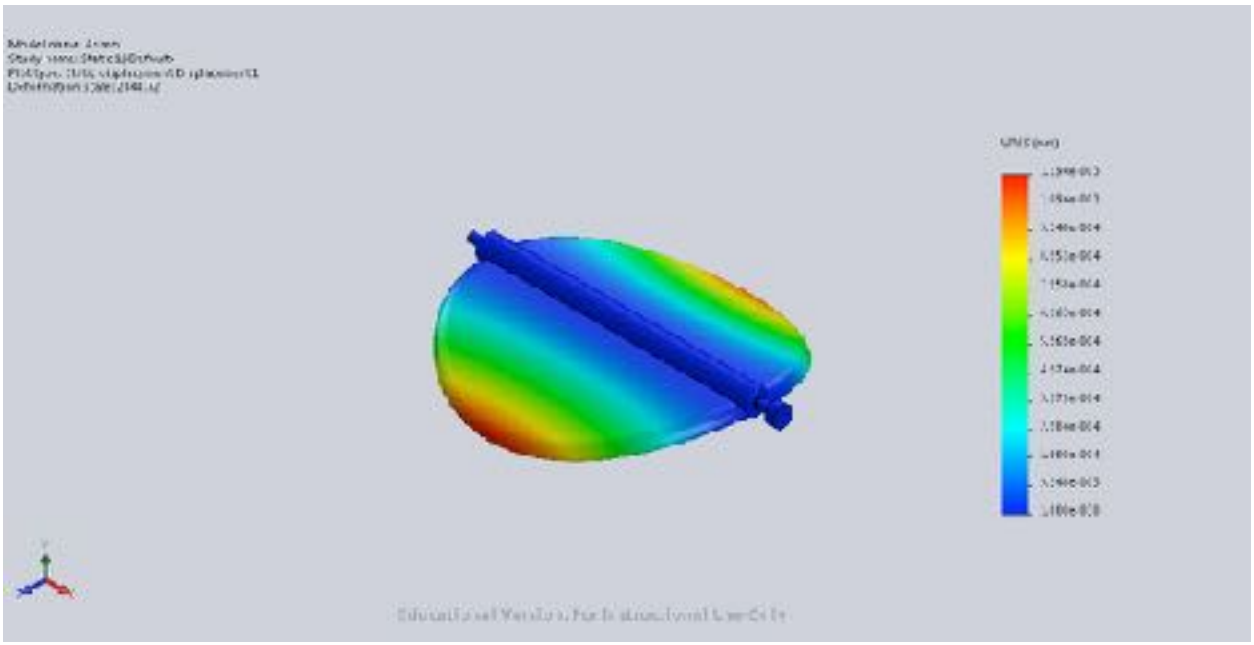

FIGURE 33: SYSTOLIC PRESSURE DISPLACEMENT ALONG TILTING DISC VALVE

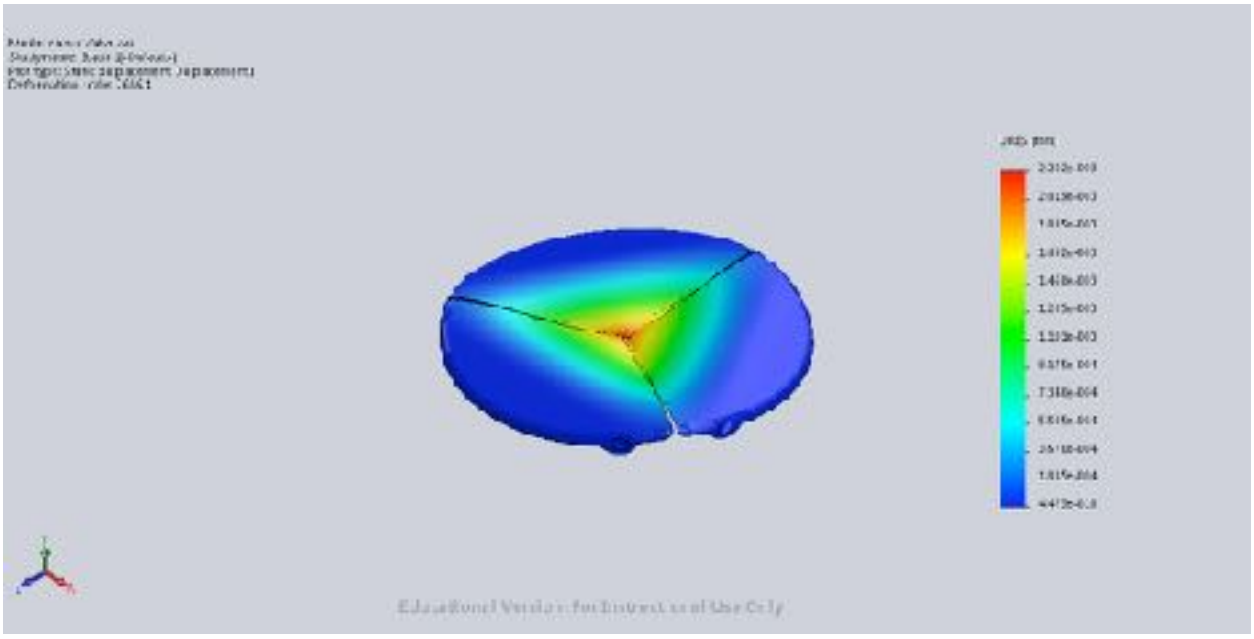

FIGURE 34: SYSTOLIC PRESSURE DISPLACEMENT ALONG TRI-LEAFLET VALVE

4.1.4 Physical Testing Analysis

Table 10 depicts the measured valves during the physical testing of the tri-leaflet valve in the exVivo heart and lung simulator. The data in this table has been converted to fit the units required for the calculations introduced in *Section 3.2.3 Experimental Testing*. The raw data that was collected on the day of testing can be found in *Table 16* in *Appendices A.2. Design Sketches,*

Drawings and Tables. The filling and discharge times were manipulated to create various systolic and diastolic pressures. As seen from *Table 2* the normal systolic and diastolic pressures of the left ventricle are 120 mmHg and 10 mmHg respectively. The valve was able to withstand systolic pressures as great as 93 mmHg and diastolic pressures as low as 15 mmHg. Due to unforeseen events with the simulator, further tests were not able to be conducted at the valve to see if it would be able to withstand pressures that were closer to physiological conditions. It can also be seen from *Table 11* that the greatest leakage of the valve is seen at high systolic pressures. This is due to the greater flow rates seen at higher systolic pressures indicating that more water is impacting the valve at these conditions.

TABLE 11: MEASURED PRESSURES AND LEAKAGE OF THE TRI-LEAFLET VALVE

Trial	Ventricular Pressure (mmHg)		Leakage: z (mmH_2O)	Filling Time (s)	Discharge Time (s)
	Systolic	Diastolic			
1.1	93.42	28.02	330	0.75	1.5
1.2	91.55	28.02	337.5	0.75	1.5
1.3	85.94	26.16	350	0.75	1.5
2.1	41.1	14.95	65	0.25	1
2.2	41.1	14.95	80	0.25	1
2.3	41.1	14.95	75	0.25	1
3.1	35.5	20.57	20	0.25	1
3.2	35.5	20.57	20	0.25	1
3.3	35.5	20.57	17	0.25	1
4.1	33.63	22.44	16	0.25	1
4.2	33.63	22.44	17	0.25	1
4.3	33.63	22.44	15	0.25	1

Table 12 summarizes the calculated results across the four different trials. At high systolic pressures, the valve was experiencing turbulent flow. At lower systolic pressures, the valve experiences laminar flows that are transitioning to turbulent flows.

TABLE 12: CALCULATED FLOW CHARACTERISTICS OF TRI-LEAFLET VALVE

Trial	Flow Rate (m^3/s)	Average Velocity: v_{avg} (m/s)	Headloss: h_f (m)	Reynold's Number: Re	Mass Flow Rate: m (kg/s)
1.1	8.33E-04	0.731	0.0004771	31718	0.831
1.2	8.33E-04	0.731	0.00048794	31718	0.831
1.3	8.33E-04	0.731	0.00050602	31718	0.831
2.1	2.5E-04	0.219	2.8192E-05	9516	0.249
2.2	2.5E-04	0.219	3.4698E-05	9516	0.249
2.3	2.5E-04	0.219	3.253E-05	9516	0.249
3.1	8.33E-05	0.0731	2.8915E-06	3172	0.0831
3.2	8.33E-05	0.0731	2.8915E-06	3172	0.0831
3.3	8.33E-05	0.0731	2.4578E-06	3172	0.0831
4.1	8.33E-05	0.0731	5.3493E-05	3172	0.0831
4.2	8.33E-05	0.0731	2.4578E-06	3172	0.0831
4.3	8.33E-05	0.0731	2.1686E-06	3172	0.0831

4.1.5 Material Selection

Material selection is based on many crucial factors: biocompatibility, fatigue, durability, thromboresistivity, strength, and resistance to wear [48]. As the production of the above design will be personalized according to a patient's requirements, there are three material options available: pure pyrolytic carbon, titanium Ti6A4V and 316L stainless steel. *Table 9* clearly and concisely summarizes the main properties of the three different materials to gain a greater insight on the differences between them. Although, all of the materials below meet the requirements to a great extent, temporary or permanent external medicinal intervention like blood thinning medications and immune system suppressing medications might be required to enhance the

material properties. Pure pyrolytic carbon is a superior choice of material but the final deliverable will be produced in 316L stainless steel due to restrictions of budget and resources.

Pure Pyrolytic Carbon- Best contender of all the materials, pyrolytic carbon has great biocompatibility. Since the material is made from only carbon and hydrogen it is well recognized by the blood platelets of the body making it less susceptive to platelet deposition and causing thrombogenesis or blood clotting. Its durability and strength comes from its structure where each layer of carbon is stacked in a disorderly manner creating distortions within layers and sub sequential interlocking [49]. It has a very low susceptibility to fatigue caused by cyclic loading and its ductility causes it to become less susceptible to cracking [49].

Titanium Ti6A4V- Titanium is another great choice of material for mechanical heart valve design. Its composition makes it a suitable choice for people with chromium or nickel incompatibility. In comparison to 316L stainless steel it has lower density making it a lighter weight material. It also has a higher tensile strength, which makes it less prone to fracture due to cyclic load. This is a great property considering that the valve has to constantly function for its lifetime. It is highly biocompatible and thromboresistant which are necessary criteria for the valve.

316 L Stainless steel- Medical grade 316L stainless steel is another viable choice for the production of the mechanical heart valve designed above. It has a density of 8 g/cm^3, which gives it high structural toughness and a tensile strength between 480-620 MPa (*Table 9*). It is highly biocompatible when coated with hypoxyapetite ceramics or other biopolymers [50]. It also withstands cyclic loading to a great extent. Since the material is an alloy of nickel and chromium, patients with allergies to these metals are advised not to use this material type for their mechanical heart valve.

4.2 Final Design Analysis

The final design described above meets most of the criteria and constraints. CFD and FEA analysis were performed on the 2D drawings of the design. Experimental testing was also done on an in-vivo heart and lung simulator to further quantify our results. The obtained results

were compared to the existing research studies and models. Some assumptions were made in order to make the design fully functional.

The design was constructed with constraints in consideration. It follows all the Class IV medical device regulations set by the health Canada. The materials suggested for the device are pure pyrolitic carbon, titanium 6Al4V and 316L stainless steel which are highly compatible materials in terms of thromboresistivity and biocompatibility *(Refer to section 4.1.1 Material Selection)*. Their low tendency for absorption of proteins and blood components make them great options for biomedical implants and other applications. All the materials are durable according to their tensile strength and fracture toughness. Although the best choice of all the three materials is pure pyrolytic carbon which is superior in every aspect, the selection of material is dependent on patient's personal requirement or doctor's diagnosis. The design is constructed in a manner that provides a complete seal in a closed position. Considering tolerances near to 0 while machining, the valve will not cause any regurgitation or leakage due to its tight seal when closed. Minimization of turbulence is another main constraint set in this project. Although, the experimental results and the CFD analysis provide a Reynolds number of 18 which signifies a laminar flow, the Velocity profile obtained from the CFD results show some turbulence under the leaflet openings (*Figure 17*). This can be due to the uneven geometry formed between the opening of the valve and the housing. This can be fixed by running more CFD simulations possibly in a 3-D CFD model and modifying the design appropriately. The tri-leaflet valve (alternative 1) that Mayet Medical designed meets the functionality of existing designs. The maximum velocity experienced by the tri-leaflet design was 152 cm/s which is comparable to the Carbomedics bi-leaflet valve and the bi-leaflet valve in the Yin et al. research study (*Table 13*).

TABLE 13: SUMMARY OF VELOCITIES FOR EXISTING DESIGNS AND MAYET MEDICALS DESIGNS

Valves	Maximum Velocity
Tri-leaflet design (Alternative 1)	152
Tilting Disc design (Alternative 2)	174
Carbomedics Bileaflet valve	143
Bjork-Shiley Mono-Leaflet valve	207
Bi-leaflet (Yin et al.)	134
Mono-leaflet valve (Yin et al.)	167

In the experimental testing, the valve was able to with stand a systolic pressure of 93.42 mmHg and a diastolic pressure of 28.02 mm Hg. The FEA analysis performed for the tri-leaflet valve reassure the fact that the materials used are durable and can withstand great amounts of stress and strain which they possibly will not have to face in a human heart. This can also be seen in *Figures 26, 28, 30 and 32* where the stresses and strains caused by the systolic and diastolic pressure are well distributed on the faces of the design.

The tri-leaflet design is contained in a uniform circular structural housing which makes it easy for suture ring placement and cardiac installation for the surgeon. The design also contains three pins that help with the movement of the leaflets, three leaflets and a housing which makes it a very precise design with minimal amount of small structural moving parts.

4.4 Assumptions

Many assumptions were made for the CFD and experimental testing. The calculations for the CFD testing were done assuming that the fluid had a laminar steady flow and it was Newtonian fluid. Also, there was turbulence in the model regardless of the discrepancy between the velocity flow map and the manually calculated values. In the experimental testing as the systolic and diastolic pressures were increased there was an increased regurgitation and leakage in the valve which is not accounted for in the results. This was caused by the great tolerance caused by the low precision in the 3D printer where the experimental prototypes were printed.

4.5 Manufacturing

When manufacturing a heart valve, it is recommended that the purchased material be in its raw state so that finishes could be added later on in the process. There are multiple suppliers of medical grade stainless steel 316L and materials can be purchased online. Stainless steel 316L can be purchased in sheet form or as pipes. For this project it would be beneficial to purchase the sheets so that the housing and leaflets could be made from the same material. On average, the price of this material ranges from $2000-$4500 US per metric ton [51]. Examples of suppliers are Brown McFarlane and Wuxi Ninhang Stainless Steel Import and Export Co., Ltd. [51], [52]. A machinist can then use the materials to form the housing, pins and leaflets. Once the valve is constructed, a polish finish must be applied to increase its resistance to corrosion, its biocompatibility and its smoothness [53]. This can be achieved through electropolishing using a magnetic field [53]. This process removes foreign material and oxides, and replaces them with a chromium oxide layer that is resistant to corrosion [53].

4.6 Costing

4.6.1 Bill of Materials

TABLE 14: BILL OF MATERIALS FOR FINAL DESIGN

Bill Of Materials	Cost/kg	Cost of Production from Selected Material
Pyrolytic Carbon [56]	$70-$90/m^2	$300
Titanium- Ti6Al4V [54]	$25 / kg	$260
316L Stainless Steel [55]	2.45/kg	$150

*Information for the bill of materials was obtained from [54]-[56].

The bill of materials is set up by research from various whole sale vendors online. The exact costs are represented in *Table 14*. Pyrolytic carbon is the most expensive material from the three and therefore will have the highest production cost.

4.6.2 Cost Analysis Manufacturing, Implementation and End of Life Costs

Table 15 shows a detailed cost analysis of the final design implementations. The development of design is calculated for each engineering working for 4 months (1 semester) at $40/hour. All of the material will be imported by wholesalers from china through Alibaba.com, the cost of different materials is listed in *Table 14* which are taken from the same website. Machining of the valve parts will be outsourced to DIACARB Machining situated in Quebec. Due to unavailability of a quote from the vendor, an estimate of the machining was obtained from cost estimation function built into the SolidWorks software. The machining costs of 1 valve will be approximately $150-$300 (depending upon the material, refer to *Table 15).*

TABLE 15: COST ANALYSIS OF FINAL DESIGN

Cost Analysis	
Development of Design	$38,400
CSA approvals and Licenses	$49,400
Manufacturing /valve	$150-$300
Assembly and packaging	$300-$400

Assembly and packaging will also be outsourced to a company called Litron Medical in USA. According to online reviews [57], [58] and existing valve prices this value was estimated between $300 and $400.

The implementation costs of the medical device are the costs set by Health Canada for obtaining the license and approvals to sell the instrument in Canada. Since, artificial heart valves are Class IV medical devices, there are strict regulations and laws involving the licenses and approvals. According to health Canada, these costs add up to about $49,400 [59], [60].

Since, the valves are required to last a lifetime, the end of life value of a valve is $0. The valve cannot be reused for any other purpose and post-death extraction of the valve is highly uncommon.

4.7 Safety

As the mechanical heart valve is meant replace an actual heart valve it must be able to withstand physiological conditions and not cause any harm to the individual it is placed in. The heart valve was designed allow a smooth flow of blood across each leaflet and be robust enough not to break under normal blood pressure. Patients should be monitored after surgery to ensure heart valve is functioning normally and not causing excessive blood cell damage (hemolysis) or blood cell clotting (thrombosis). Mild, compensated hemolysis associated with mechanical heart valves is not uncommon even in the current era. Severe hemolysis is rare, however, and is usually associated with a paravalvular leak, a leakage through the heart valve [61].Anticoagulant medication is prescribes to help prevent thrombosis and will be taken for the rest of the patients life. Patients should be aware that anticoagulation medication helps delay clots by delaying the blood coagulation process as any cuts or scrapes will bleed longer than usual. Recovery for patients who undergo heart valve replacement surgery takes around 8 to 12 weeks [61]. Patients should also take note that as with any surgery complications can always arise and can lead to more surgery and possibly death [61].

4.8 Society Implications

The need for heart valve replacement surgery has increased the need for artificial heart valves. The tri-leaflet heart valve that was designed is intended to replace an individual's existing heart valve by providing a more physiologically similar mechanical heart valve than existing mechanical valves currently in use. By having a three leaflet design this valve will allow blood to flow like it would in an actual valve. Using CFD analysis allowed the leaflets to be designed so that they would reduce cavitation, thrombosis and hemolysis by providing good hemodynamics with very low aerodynamic resistance. This design will be constructed out of 316L medical grade stainless steel which is cheaper than a titanium alternative but less biocompatible.

4.9 Risks and Uncertainties

Most mechanical heart valves have to be designed to prevent hemolysis, (hemolytic anemia) low red blood cell count, bleeding, infection, thrombosis, embolism, bleeding and endocarditis [62]. Replacement of these valves at an older age carries a higher risk of mortality,

about 11.5% less than 70 years of age, 17.3% greater than 70 years of age and 32.0% at greater than 80 years of age [62]. Failure usually occurs from 5 to 15 years after the implant [62]. One of the biggest risks associated with all the designs presented is the breakage of the leaflets. A potential concern with mechanical heart valves is that the leaflets could either impede blood flow to the heart or get stuck inside the heart itself. Another risk is if the leaflets do not function properly and allow too much leakage. This could cause a significant damage to the heart, could impede blood flow and could cause the patient to experience a heart attack [20]. Patients with mechanical heart valves are usually prescribed anticoagulant medication or blood thinners. Blood thinners do not thin the blood but increase the amount of time it takes for the blood to clot. In some instances patients may suffer from unexpected bleeding from these medications. It is also possible that blood could clot on the valve itself. These blood clots could cause thrombosis, where the clots could grow large enough to affect the functionality of the valve or cause a thromboembolism, where the clot could break loose and travel with the blood to another part of the body and block circulation [20]. It is very important that doctors monitor the patient's blood and make sure a correct amount of anticoagulant medication is prescribed to the patient. With any surgically invasive surgery there is always a possibility of infection, especially with a foreign device being placed inside. While this is not a common occurrence with prosthetic heart valves there is still a slight possibility of this occurring after surgery.

5.0 Conclusions

The chosen tri-leaflet design assesses some of the issues with current designs and is comparable to the results of previous studies. The important aspects of the design are the curvature of the leaflets, the containment of the leaflets within the housing, the inclusion of stoppers and the overall rounding of edges. The leaflets were curved to prevent the leaflets from sticking to one another or to the housing during movement while still creating a seal to prevent backflow or leakage. Stoppers were also added to prevent over rotation so that backflow is minimized. The leaflets were contained within the housing of the valve to ensure that minimal impact occurs to other anatomical cardiac structures. All the edges of the valve were rounded or

filleted to increase the overall smoothness of the valve and therefore decreasing turbulence across the valve.

The maximum velocity obtained from the valve through computational fluid dynamic modelling was 152 cm/s. This is comparable to the Carbomedics bi-leaflet valve and the bi-leaflet valve in the Yin et al. research study. A future design could include modification to the range of leaflet motion to decrease turbulence around the leaflet. This would decrease the risk of coagulation and platelet activation.

The maximum stress exerted over the area of the valve through finite element analysis was 289.556 kN/m^2. The valve also showed a more distributed stress and strain concentration along its leaflets than the tilting disc valve. This can be explained by the distribution of the load across three leaflets in the tri-leaflet design as opposed to the concentration of load on the sole disc of the tilting disc valve.

Physical testing in the ex vivo heart and lung simulator was done with a 3-D printed model of the tri-leaflet valve in ABS plastic. The valve was able to operate under pressures that were close to physiological pressures. The results of this test indicated that while turbulent flows were seen at high systolic pressures, the flow was in a transition state from laminar to turbulent at low systolic and diastolic pressures. Further comparisons to other valves would need to be made to compare the Reynold's number against the tri-leaflet valve.

If further development of the valve was to be conducted in order to make it ready for in vivo implantation, the following estimated costs may apply. The development of the design would cost approximately $38 400. The valve would also have to meet certain standards and approvals such as CSA approvals and ethics. These approvals along with required licenses would cost approximately $49 400. The estimated manufacturing cost per valve would be $300 while the estimated cost for assembling and packaging would be $400.

The final deliverable of this project is a 3-D printed model in medical grade stainless steel 316L. This material was chosen for its durability and biocompatibility. The application of a polished finish should be added to increase the materials biocompatibility and its resistance to

corrosion. A polished finish would also increase the overall smoothness of the valve, therefore reducing the turbulence across the valve.

6.0 Recommendations

2-D modelling was done for both the computational fluid dynamics (CFD) and finite element analysis (FEA) models due to the limitations in memory for the software at the University of Guelph. It is recommended that 3-D modelling be done to develop a more accurate analysis of flow across the valve. Due to limitations in time for the project, the 3-D printed medical grade stainless steel model 316L was not tested in the ex vivo heart and lung simulator. It is recommended that this model also be tested in the simulator and also undergo cyclic loading fatigue testing to estimate its longevity. The experiment was also conducted using water as the fluid flowing across the valve. It is recommended that for future testing a fluid similar to blood composition be used to analyze the interaction of the fluid to the material. It is also recommended that further redesign be completed to further decrease the turbulence between the housing and pin. The final deliverable for this project was a prototype of the valve 3-D printed from medical grade stainless steel 316L. To account for patients that may be sensitive to the composition of stainless steel, it is also recommended to conduct simulations on a titanium 3-D printed model.

7.0 References

[1] Heart and Stroke Foundation. (2011, March 1). *Heart Disease: Valve Disorders* [Online]. Available: http://www.heartandstroke.com/site/c.ikIQLcMWJtE/b.3484083/k.2A3F / Heart_disease_Valve_disorders.htm

[2] MedicineNet. (n.d.). *Heart Valve Disease Symptoms, Causes, Treatment: How are valve diseases diagnosed?* [Online]. Available: http://www.medicinenet.com/heart_valve_disease/page4.htm

[3] E. N. Marieb, "The Cardiovascular System," in *Essentials of Human Anatomy and Physiology*, 10th ed. San Francisco: Pearson Education Inc., 2012, ch. 11, pp. 357-397.

[4] J. K. J. Li, "Functional Properties of Blood" in *Dynamics of the Vascular System*, River Edge: World Scientific, 2004, ch. 2, sec. 3, pp. 30-35.

[5] B. Phibbs, "Structure and Function of the Normal Heart" in *The Human Heart: A Basic Guide to Heart Disease*, 2nd ed. Philadelphia: Lippincott Williams and Wilkins, 2007, ch. 1, pp. 1-5.

[6] B. Phibbs, "Valves of the Heart" in *The Human Heart: A Basic Guide to Heart Disease*, 2nd ed. Philadelphia: Lippincott Williams and Wilkins, 2007, ch. 2, pp. 6-10.

[7] L. Axel, "Papillary muscles do not attach directly to the solid heart wall," *Circulation*, vol. 109, no. 25, pp. 3145-3148, June, 2004.

[8] S. Westaby, R. B. Karp, E. H. Blackstone and S. P. Bishop, "Adult human valve dimensions and their surgical significance," The American Journal of Cardiology, vol. 53, no. 4, pp. 552-556, Feb. 1984.

[9] B. Phibbs, "The Functioning of the Normal Heart" in The Human Heart: A Basic Guide to Heart Disease, 2nd ed. Philadelphia: Lippincott Williams and Wilkins, 2007, ch. 5, pp. 13-20.

[10] University of Notre Dame. (2004, April 22). *Physics in Medicine* [Online]. Available: http://www3.nd.edu/~nsl/Lectures/mphysics/

[11] E. Rabkin-Aikawa, J. E. Mayer and F. J. Schoen, "Heart valve regeneration," *Adv Biochem Engin/Biotechnol*, vol. 94, pp. 141-179, 2005.

[12] J. E. Barber, F. K. Kasper, N. B. Ratliff, D. M. Cosgrove, B. P. Griffin and I. Vesely, "Mechanical properties of myxomatous mitral valves," *Journal of Thoracic and Cardiovascular Surgery*, vol. 122, no. 5, pp. 955-962, 2001.

[13] V. L. Brashers, "Alterations of Cardiovascular Function," in *Understanding Pathophysiology*, ed. 4, St. Louis: Mosby Elsevier, 2008, ch. 23, pp. 606-675.

[14] P. Libby, R. O. Bonow, D. L. Mann, D. P. Zipes, "Valvular Heart Disease," in *Braunwald's Heart Disease: A Textbook of Cardiovascular Medicine*, ed. 8, Elsevier, 2008, ch. 62, pp. 1625-1712.

[15] M. Enriquez-Sarano, J. F. Avierinos, L. H. Ling, F. Grigioni, D. Mohty and C. Tribouilloy, "Surgical treatment of degenerative mitral regurgitation: should we approach differently patients with flail leaflets of simple mitral valve disease," in *Pathophysiology, Evaluation and Management of Valvular Heart Diseases,* vol. 2, J. S. Borer and O. W. Isom, Eds. Basel, Switzerland: Karger, 2004, vol. 41, pp. 95-107.

[16] M. Berger, "Natural history of mitral stenosis and echocardiographic criteria and pitfalls in selecting patients for balloon valvuloplasty," in *Pathophysiology, Evaluation and Management of Valvular Heart Diseases,* vol. 2, J. S. Borer and O. W. Isom, Eds. Basel, Switzerland: Karger, 2004, vol. 41, pp. 87-94.

[17] American Heart Association. (2014, March 26). Options and Consideration for Heart Valve Surgery [Online]. Available: http://www.heart.org/HEARTORG/Conditions/More/HeartValveProblemsandDise ase/Options-and-Considerations-for-Heart-Valve-Surgery_UCM_450787_Article.jsp

[18] R. Hetzer, J. S. Rankin and C. A. Yankah, "Preface: A success story in medicine," in Mitral Valve Repair, Berlin, Germany: Springer, 2011, pp. v-vi.

[19] V. L. Gott, D. E. Alejo and D. E. Cameron, "Mechanical heart valves: 50 years of evolution," *The annals of Thoracic Surgery*, vol. 76, no. 6, pp. 2230-2239, 2003.

[20] G. L. Grunkemeier and S. H. Rahimtoola, "Artificial heart valves," Annu. Rev. Med., vol. 41, no. 1, pp. 251-263, 1990.

[21] H. Mohammadi and K. Mequanint, "Prosthetic aortic heart valves: modeling and design," *Medical engineering and physics*, vol. 33, no. 2, pp 131-147, 2011.

[22] M. W. King, B. S. Gupta and R. Guidoin, "Biotextiles as Percutaneous Heart Valves," in *Biotextiles as Medical Implants*, Cambridge, UK: Woodhead Publishing Limited, 2013, ch. 16, sec. 3, pp. 491-492.

[23] M. W. King, B. S. Gupta and R. Guidoin, "Hemostatic Wound Dressings," in *Biotextiles as Medical Implants*, Cambridge, UK: Woodhead Publishing Limited, 2013, ch. 19, sec. 4, pp. 573-574.

[24] P. Boloori-Zadeh, S. C. Corbett and H. Nayeb-Hashemi, "Effects of fluid flow shear rate and surface roughness on the calcification of polymeric heart

leaflet valve," *Materials Sci. and Eng.*, vol. 33, no. 5, pp. 2770-2775, 2013.

[25] T. E. Claiborne, M. J. Slepian, S. Hossainy, D. Bluestein, "Polymeric trileaflet prosthetic heart valves: evolution and path to clinical reality," *Expert Review of Medical Devices,* vol. 9, no. 6, pp. 577, 2012.

[26] B. D. Ratner, A. S. Hoffman, F. J. Schoen, J. E. Lemons, "Pyrolytic Carbon for Long-Term Medical Implants," in *Biomaterials Science: An Introduction to Materials in Medicine Third Edition*, San Diego: Elsesvier Academic Press, 2004, ch. 2, sec. 11, pp. 170-181.

[27] P. A. Iaizzo, R. W. Bianco, A. J. Hill, J. D. St. Louis, "Heart Valve Substitute Use Conditions," in *Heart Valves from Design to Clinical Implantation*, New York: Springer Sciences and Business Media, 2013, ch. 12, sec. 3, pp. 286-308.

[28] K. Jozwik and A. Karczemska, "The new generation Ti6Al4V artificial heart valve with nanocrystalline diamond coating on the ring and with Delrin disc after long-term mechanical fatigue examination," *Diamond and Related Materials,* vol. 6, pp. 1004-1009, Jan. 2007.

[29] S. V. Bhat, "Metals," in *Biomaterials Second Edition*, Middlesex, U.K.: Alpha Science International Ltd, 2005, ch. 3, sec. 2, pp. 27-29.

[30] W. D. Callister and D. G. Rethwisch, "Appendix B: Properties of Selected Engineering Materials," in *Materials Science and Engineering 8th Edition*, USA: John Wiley and Sons, Inc., 2010, Appendix B, pp. A3-A30.

[31] *Materials Science and Engineering Handbook,* Third ed., CRC Press LLC, Boca Raton, Florida, 2001.

[32] D. S. Gelles, R. K. Nanstad, A. S. Kumar and E. A. Little, "Fracture Toughness of Irradiated Candidate Materials for Iter First Wall/Blanket Structures," in *Effects of Radiation on Materials 17th Volume*, West Conshohocken, PA: American Society for Testing and Materials, 1996, pp. 945-963.

[33] G. Salhotra, V. Bajpai and R. K. Singh, "Finite Element Modeling of Orthogonal Cutting of Pyrolytic Carbon," *ASME 2011 international Manufacturing Science and Engineering Conference*, vol. 1, pp. 153-160, June, 2011.

[34] *Technical Data Sheet of SS 316L*, 1 ed., Hamilton Precision Metals, PA.

[35] SolidWorks. (2014) Computational fluid dynamics (CFD) [Online]. Available: http://www.solidworks.com/sw/products/simulation/computational-fluid-dynamics.htm

[36] S. G. D. Kelly, “Computational fluid dynamics insights in the design of mechanical heart valves,” Artificial Organs, vol. 26, no. 7, pp, 608-613, 2002.

[37] SolidWorks. (2014) Finite element analysis [Online]. Available: http://www.solidworks.com/sw/products/simulation/finite-element-analysis.htm

[38] A. N. Smuts, D. C. Blaine, C. Scheffer, H. Weich, A. F. Doubell and K. H. Dellimore, “Application of finite element analysis to the design of tissue leaflets for a percutaneous aortic valve,” Journal of the Mechanical Behaviour of Biomedical Materials, vol. 4, no. 1, pp. 85-98, 2011.

[39] S. M. Wells, T. Sellaro and M. S. Sacks, “Cyclic loading response of bioprosthetic heart valves: effects of fixation stress state on the collagen fiber architecture,” *Biomaterials*, vol. 26, no. 15, pp. 2611-2619, 2005.

[40] Ametek, Inc. (2010). *Rockwell Hardness Testing* [Online]. Available: http://www.hardnesstesters.com/Applications/Rockwell-Hardness-Testing.aspx

[41] B. Glasmacher, E. Nellen, H. Reul and G. Rau, “In vitro hemocompatibility testing of new materials for mechanical heart valves,” *Materialwissenschaft und Werstofftechnik*, vol. 30, no. 12, pp. 806-808, 1999.

[42] Medical Devices Regulations (SOR/98-282) (2011, December 16/ Rev 2014, September 01), Schedule 1 (Section 6) Classification rules for medical devices [Online]. Available: http://laws lois.justice.gc.ca/eng/regulations/sor-98-282/page-23.html#h-68

[43] W. Yin, Y. Alemu, K. Affeld, J. Jesty, D. Bluestein, “Flow-induced platelet activation in bileaflet and monoleaflet mechanical heart valves,” in *Annals of Biomedical Engineering,* vol. 32, no. 8, pp. 1058-1066, 2004.

[44] D. Bluestein, L. Niu, R. T. Schoephoerster, M.K. Dewanjee, “Fluid Mechanics of Arterial Stenosis: Relationship to the Development of Mural Thrombus,” in *Annals of Biomedical Engineering,* Vol. 25, 1997. pp. 344-356.

[45] B. Guest, L. Arroyo, L. Viel, C. Kerr, J. Runciman, “Ex Vivo Equine Heart and Lung Perfusion system,” Journal of Biomechanical Engineering ASME, Guelph, 2014.

[46] F. M. White, “Laminar Fully Developed Pipe Flow,” in *Fluid Mechanics Seventh Edition*, New York: McGraw Hill, 2011, ch. 6, sec. 4, pp. 357-359.

[47] P. J. Daley, K. B. Sagar, L. S.Wann, “Doppler echocardiographic measurement of flow velocity in the ascending aorta during supine and upright exercise,” in *Br Heart F,* vol. 54, pp. 562-567, 1985.

[48] *Pyrolytic Carbon for Biomedical Applications.* (2014). [Online]. Available: http://www.azom.com/article.aspx?ArticleID=1463

[49] Dr. Irene Turner, D (2014)., *Case Study - Mechanical Heart Valves*. [Online]. Available: http://classroom.materials.ac.uk/caseHeart.php

[50] Hermawan, H., Ramdan, D., Djuansjah, J.R., *Biomedical Engineering - From Theory to Application*. InTech ;.2011 Available: http://cdn.intechopen.com/pdfs- wm/18658.pdf

[51] Alibaba.com. (2014). *Medical Grade Stainless Steel 316L Suppliers* [Online]. Available: http://www.alibaba.com/corporations/medical_grade_stainless_steel_316l.html

[52] Brown McFarlane. *316/316L Stainless Steel*. [Online]. Available: http:// www.brownmac.com/products/stainless-steel-plate/Stainless-Steel-316- and-316l.aspx

[53] R. Rokicki, T. Hryniewicz and K. Rokosz, “Corrosion characteristics of medical-grade AISI type 316L stainless steel surface after electropolishing in a magnetic field,” *Corrosion,* vol. 64, no. 8, pp. 660-665, 2008.

[54] Alibaba.com. (2014). [Online]. Available: http://www.alibaba.com/product- detail/ Titanium-ti-6al-4v_995739663.html?s=p

[55] Alibaba.com. (2014). [Online]. Available: http://www.alibaba.com/product- detail/316l-stainless-steel-price-316-stainless_1926578635.html

[56] Alibaba.com. (2014). [Online]. Available: http://www.alibaba.com/product- detail/High-Pyrolytic-Carbon-Fiber-PGS-Graphite_1285887244.html?s=p

[57] Capretz & Associates. (2014). *St. Jude Silzone Heart Valve Recall*. [Online]. Available: http://www.capretz.com/st-jude-silzone- valve/?gclid=COzf6fnMo8ICFfEF7AodRycAww

[58] Litron Inc. (2011). [Online]. Available: http://www.litron.com/

[59] *Fees for The Examination of Medical Device Licence Applications.* (2014). [Online]. Available: http://laws-lois.justice.gc.ca/eng/regulations/SOR-2011-79/page- 12.html#h-29

[60] *Schedule 7*. (2014). [Online]. Available: http://laws-lois.justice.gc.ca/eng/regulations/SOR-2011-79/page-23.html#h-49

[61] L. Dasi, H. A. Simon, P. Sucosky and A. P. Yoganathan, “Fluid mechanics of artificial heart valves” Clin Exp Pharmacol Physiol. Feb 2009; 36(2): 225–237.

[62] Division of adult Cardiothoracic surgery (2014 ,January 11), *Heart Valve disease* [Online]. Available: http://cardiac.surgery.ucsf.edu/conditons--procedures/aortic-- mitral-valvedisease.aspx

Appendices

A.1: Detailed Design Calculations

A.1.1 Physical Testing Sample Calculations

These calculations are conducted for trial 1.1

Poiseuille's Relationship

1. Determine the average velocity across the valve.

$$v_{avg} = \frac{Q}{\pi r^2}$$

$$v_{avg} = \frac{0.000833\ m^3/s}{\pi(0.01905\ m)^2}$$

$$v_{avg} = \frac{0.000833\ m^3/s}{\pi(0.01905\ m)^2}$$

$$v_{avg} = 0.73\ m/s$$

2. Determine the change in HGL. (Note: since the outlet tube was held at an angle of approximately 180 degrees z = L)

$$Q = \frac{\pi \rho g d^4 h_f}{128 \mu L}$$

$$h_f = \frac{128 \mu L Q}{\pi \rho g d^4}$$

$$h_f = \frac{128(8.76 \times \frac{10^{-4} kg}{ms})(0.33\ m)(0.000833 \frac{m^3}{s})}{\pi(996.813 \frac{kg}{m^3})(9.81 \frac{m}{s^2})(0.0381\ m)^4}$$

$$h_f = 0.0004771\ \text{m}$$

3. Determine the Reynold's number.

$$Re = \frac{0.73 \frac{m}{s}(0.0381 m)}{(8.784 \times 10^{-7})}$$

Conservation of Mass

4. Determine the mass flow rate across the valve.

$$mass flow rate = \rho_1 A_1 V_1 = \rho_2 A_2 V_2$$

$$mass flow\ rate = (996.813\frac{kg}{m^3})(1.14 \times 10^{-3} m^2)(0.73\frac{m}{s})$$

$$mass flow\ rate = 0.831\frac{kg}{s}$$

A.2: Design Sketches, Drawings and Tables

A.2.1 Sketches and SolidWorks Model of Tilting Disc Valve

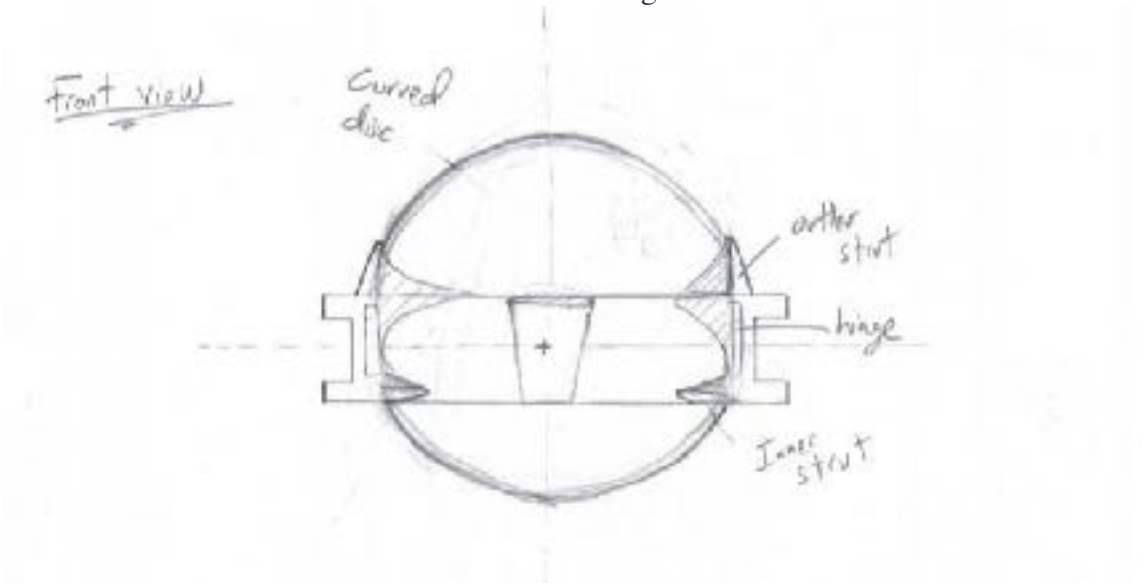

FIGURE 35: SKETCH OF FRONT VIEW OF TILTING DISC VALVE

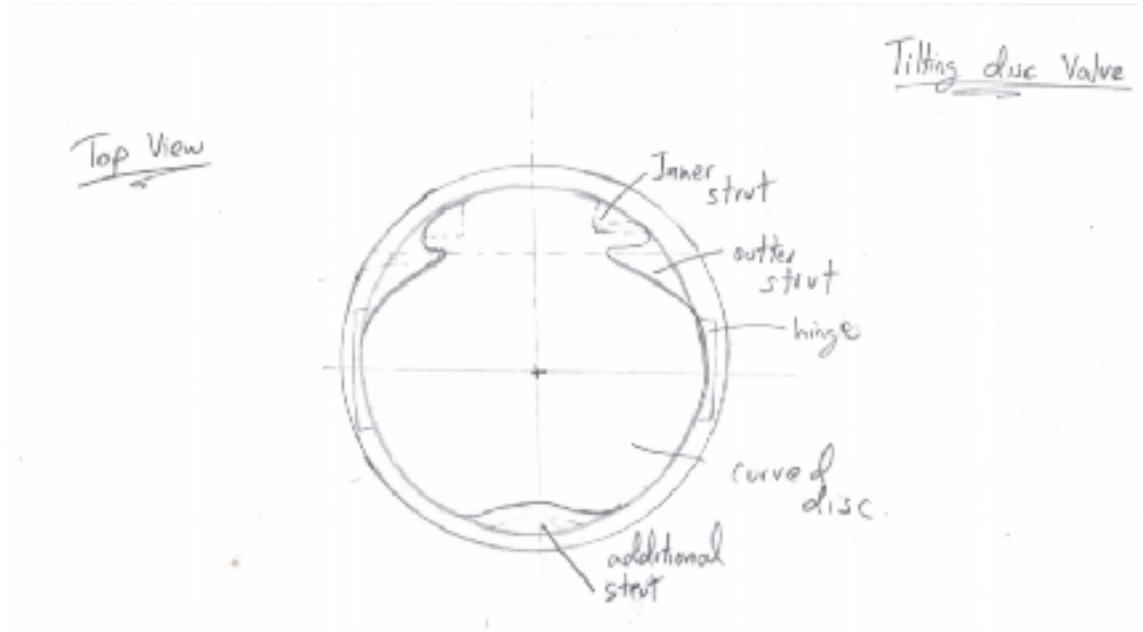

FIGURE 36: SKETCH OF TOP VIEW OF TILTING DISC VALVE

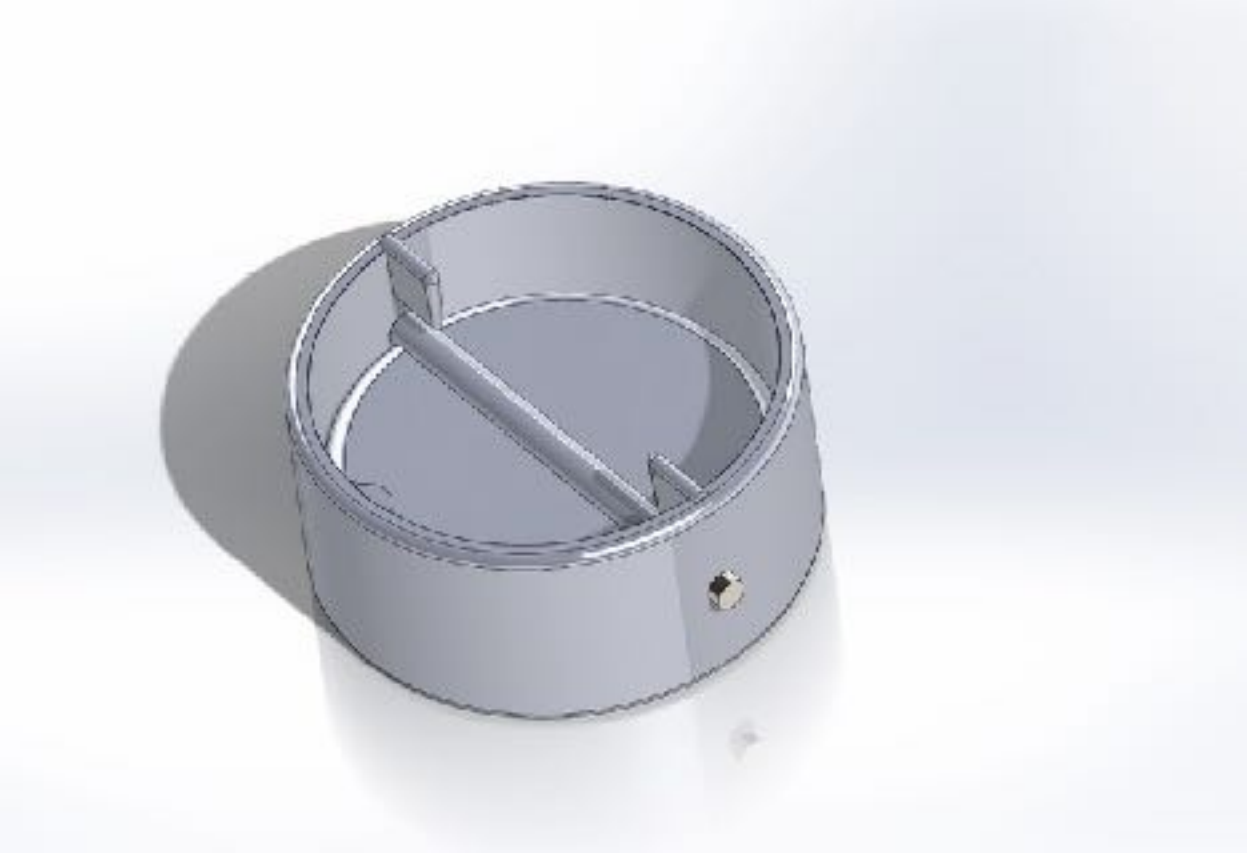

FIGURE 37: SOLIDWORKS MODEL OF TILTING DISC VALVE

A.2.2 Raw Results of Physical Testing of Tri-Leaflet Valve

TABLE 16: RAW RESULTS FROM HEART-LUNG SIMULATOR

Time on Endoscope Video	Ventricular Pressure (in H_2O)		Height: z (mm H_2O)	Flow Rate (L/min)	Filling Time (s)	Discharge Time (s)
	Systolic	Diastolic				
15:18	50	15	difference: 330 from valve: 510	50	0.75	1.5
15:22	49	15	difference: 330 from valve: 530 difference: 345 from valve: 570	50	0.75	1.5
15:28	46	14	difference: 350 from valve: 560	50	0.75	1.5
15:45	22	8	backflow from one pulse: 65	15	0.25	1
15:46	22	8	backflow from one pulse: 80	15	0.25	1
15:47	22	8	backflow from one pulse: 75	15	0.25	1
15:48	19	11	difference: 20	< 5	0.25	1
	19	11	difference: 20	< 5	0.25	1
15:50	19	11	difference: 17	< 5	0.25	1
15:52	18	12	from leaflet 370 difference: 16	< 5	0.25	1
	18	12	difference: 17	< 5	0.25	1
	18	12	difference: 15	< 5	0.25	1

A.3: Reference Material

A.3.1 Reference Material from SolidWorks

TABLE 17: MATERIAL PROPERTIES FOR STAINLESS STEEL 316L

Material Properties for 316L stainless steel
Name: AISI Type 316L stainless steel
Model type: Linear Elastic Isotropic
Default failure criterion: Max von Mises Stress
Yield strength: 1.7e+008 N/m^2
Tensile strength: 4.85e+008 N/m^2
Elastic modulus: 2e+011 N/m^2
Poisson's ratio: 0.265
Mass density: 8027 kg/m^3
Shear modulus: 8.2e+010 N/m^2
Thermal expansion coefficient: 1.65e-005 /Kelvin

*These properties were obtained from SolidWorks database.

A.3.2: Schematics for Original Use of Heart and Lung Simulator

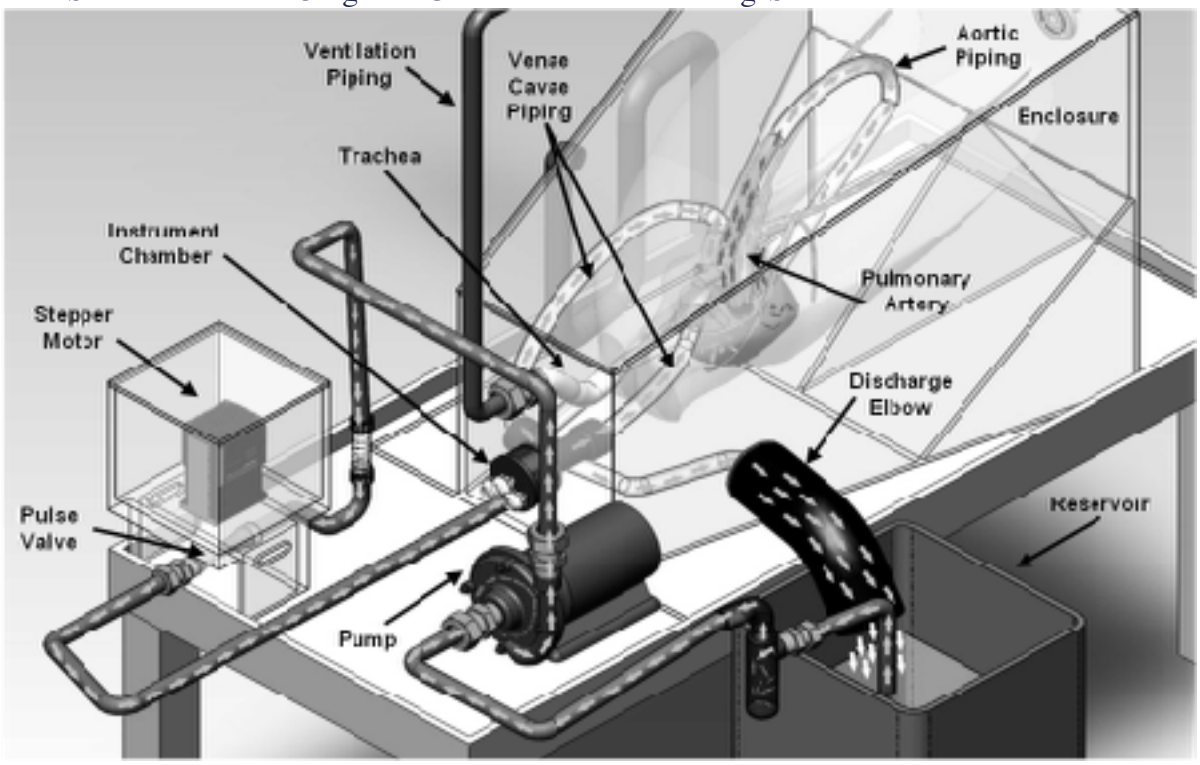

*This image was obtained from studies from [ref 20 of interim].

FIGURE 38: ILLUSTRATION OF EVHLPS WITH HEART AND LUNGS INSTALLED

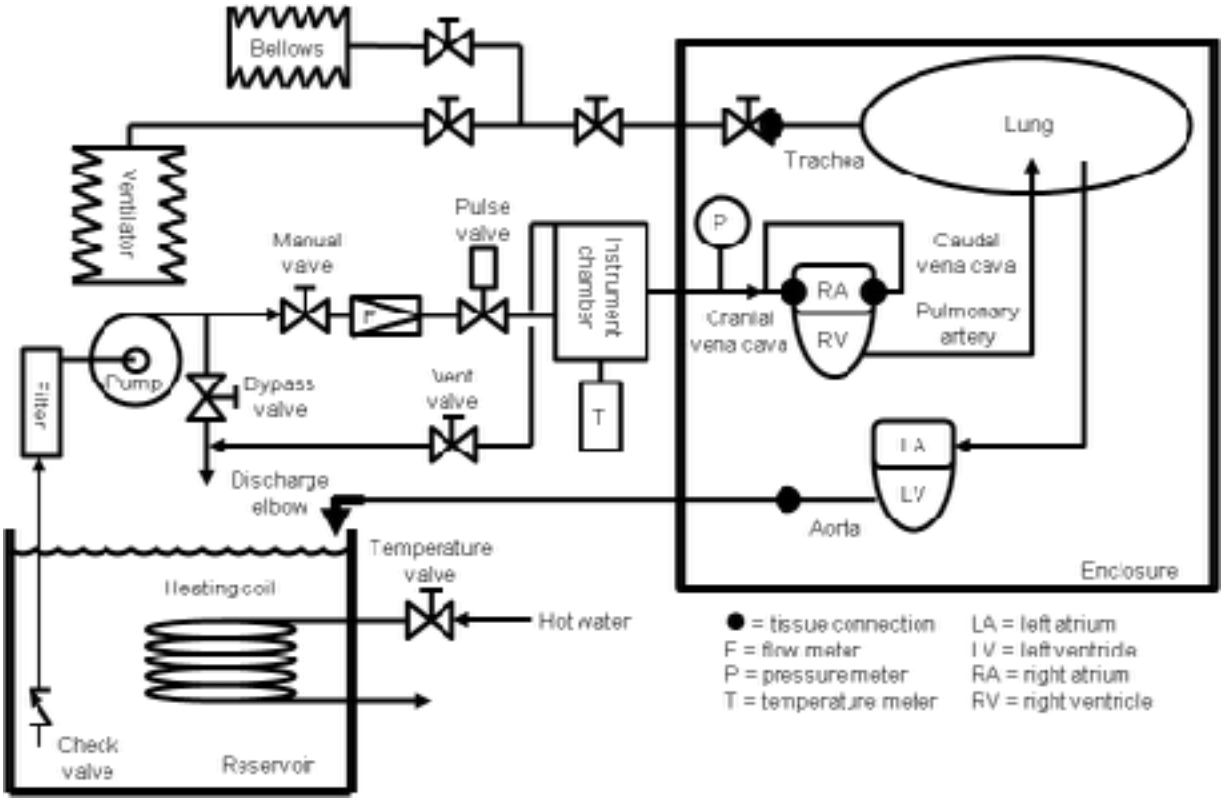

*This image was obtained from studies from [ref 20 of interim].

FIGURE 39: EVHLPS SCHEMATIC

A.4: Updated Work Plan

TABLE 18: UPDATED WORK PLAN

Milestones/ Deliverables	Target Completion Date	Description
3D SolidWorks Model	October 15th 2014.	The tri-leafelt design was created on a 1:2 scale for experimental purposes.
ABS Printed Models	October 20th 2014.	The designs were printed to evaluate them in the heart and lung simulator.
Redesign/Editing	October 30th, 2014.	Changes were made to the designs to be compatible with the simulator.
Test Designs in the Simulator	November 7th, 2014.	The designs suffered leakage around housing due to a broken seal.
Redesign for Simulator	November 15th, 2014.	The design housings were redesigned for implementation in the simulator without leakage.
Test Valves in Heart and Lung Simulator	November 20th, 2014.	The designs were placed in the simulator and experimental data was collected focusing on flow rate and associated pressures.
2D Computational Fluid Dynamic Analysis	November 20th, 2014.	This analysis technique was used in order to view the fluid flow through a cross section of the valves. Velocity magnitude and flow patterns were the focus of the technique.
Finite Element Analysis Model	November 20th, 2014.	This was used to view loading on valve components such as the leaflets, or the pins/hinges.
Final Design Model	November 27th, 2014.	Tri-leaflet design was chosen and redesigned to human vessel parameters while maintaining pin diameter.
Poster Prep and Presentation	November 27th, 2014.	Poster was created including design description and results. It was presented in the UoG Engineering building on the completion date.
3D Print Final Prototype in Stainless Steel	November 28th, 2014.	Final design was submitted for printing in 316L stainless steel
Final Design Report	December 1st, 2014.	Final report submission of design including stainless steel model.